

Supplemental information

Subgenomic flavivirus RNA binds the mosquito DEAD/H-box helicase ME31B and determines Zika virus transmission by *Aedes aegypti*

Giel P. Göertz*, Joyce W.M. van Bree*, Anwar Hiralal*, Bas M. Fernhout*, Carmen Steffens*, Sjef Boerent†, Tessa M. Visser‡, Chantal B.F. Vogels‡§, Sandra R. Abbo*, Jelke J. Fros*, Constantianus J.M. Koenraadt‡, Monique M. van Oers*, Gorben P. Pijlman*

* Laboratory of Virology, Wageningen University & Research, Droevedaalsesteeg 1, 6708 PB, Wageningen, The Netherlands

† Laboratory of Biochemistry, Wageningen University & Research, Stippeneng 4, 6708 WE, Wageningen, The Netherlands

‡ Laboratory of Entomology, Wageningen University & Research, Droevedaalsesteeg 1, 6708 PB, Wageningen, The Netherlands

§ Department of Epidemiology of Microbial Diseases, Yale School of Public Health, 60 College Street, New Haven, CT 06510, USA.

Supplemental Material and Methods

Cell lines

African green monkey kidney Vero E6 cells (ATCC CRL-1586) were cultured in Dulbecco's modified Eagle medium (DMEM; Gibco) supplemented with 10% foetal bovine serum (FBS; Gibco), penicillin (100 U/ml; Sigma-Aldrich) and streptomycin (100 µg/ml; Sigma-Aldrich) and incubated at 37 °C with 5% CO₂. For experiments, Vero cells were incubated in DMEM-HEPES (Gibco) supplemented with penicillin and streptomycin (DMEM-supplemented). For experiments with mosquito samples, additional Fungizone (50 µg/ml) and gentamycin (50 µg/ml; Life Technologies) were added (DMEM-complete). *Aedes aegypti* Aag2 and *Ae. pseudoscutellaris* AP-61 cells were cultured in Schneider's Drosophila medium (Lonza) supplemented with 10% FBS and incubated at 28 °C. *Ae. albopictus* C6/36 (ATCC CRL-1660) and *Ae. albopictus* U4.4 cells were cultured in Leibovitz L-15 medium (Gibco) supplemented with 10% FBS, 2% tryptose phosphate broth (Gibco) and 1% nonessential amino acids (Gibco) and incubated at 28 °C. During experiments gentamicin (50 µg/ml) was added to the culture medium of Aag2 and C6/36 cells.

Generation of ZIKVΔSF1 and ZIKVΔSF1+2

The NS5-3'UTR region was PCR amplified using primers 1,2 (All primers used are listed in Table S1) and cloned into pJET1.2 (Thermo Scientific) to create pJET1.2-ZIKV^{NS5-3'UTR}. Site-directed mutagenesis using pJET1.2-ZIKV^{NS5-3'UTR} as template and primers 3,4 was used to mutate the pseudoknot in SL-I (GGGG10423CCCC) to generate pJET1.2-ZIKV^{NS5-3'UTRΔSF1}. Subsequently, site-directed mutagenesis using pJET1.2-ZIKV^{NS5-3'UTRΔSF1} as template and primers 5,6 was used to mutate the pseudoknot in SL-II (CGG10503ACC) to generate pJET1.2-ZIKV^{NS5-3'UTRΔSF1+2}. The NS5-3'UTR region of pJET1.2-ZIKV^{NS5-3'UTRΔSF1} and pJET1.2-ZIKV^{NS5-3'UTRΔSF1+2} was cloned as BstBI/Fsel (New England Biolabs (NEB)) fragment into pZIKV_{IC} to generate pZIKVΔSF1 and pZIKVΔSF1+2. pZIKV_{IC}, pZIKVΔSF1 or ZIKVΔSF1+2 were linearized by AgeI digestion and used as template for SP6-based *in vitro* RNA

transcription (NEB), with m⁷G_{ppp}G RNA cap structure analogue (NEB) following the manufacturer's protocol.

Recently colonized *Aedes aegypti* mosquitoes from French Guiana (ir0115) and Kenya.

Eggs of *Aedes aegypti* strain ir0115 (French Guiana, obtained through European Union Horizon 2020 Research Infrastructure Program Infravec2: <https://infravec2.eu>) were shipped from Institut Pasteur, French Guiana to the insectaries of the Laboratory of Entomology at Wageningen University, the Netherlands. This colony was recently established (January 2015) and is now in its 16th generation. Mosquitoes were reared in a climate controlled room at 28 °C and 40% relative humidity with a 12/12h light/dark cycle. Larvae were reared in plastic containers and fed twice a week with Tetramin Baby fish food (Melle, Germany). Pupae were allowed to emerge in the plastic trays covered with nylon stockings and afterward were collected and kept in 30 cm³ Bugdorm cages. Adults were fed ad libitum daily with a 6% glucose solution on cotton wool. Adult females were fed with human blood (Sanquin Blood Supply Foundation, Nijmegen, The Netherlands) for keeping up the rearing, using a Hemotek PS5 membrane feeding system (Discovery workshops, UK) at 38 °C. Adult female mosquitoes were transported to the BSL3 laboratory at Wageningen University, the Netherlands.

Eggs of *Aedes aegypti* mosquitoes, which were collected in Rabai (Kenya) in the winter of 2018, were hatched (F1) at the University of Pavia, Italy. At adulthood, mosquitoes were checked for infection using Flavivirus degenerate primers (1). No infection was detected, and mosquitoes were reared under constant conditions, at 28 °C and 70-80% relative humidity with a 12/12h light/dark cycle. Larvae were reared in plastic containers, at a controlled density to avoid competition for food. Food was provided daily in the form of fish food (Tetra Goldfish Gold Colour). Adults were kept in 30 cm³ cages and fed with cotton soaked in 0.2 g/ml sucrose as a carbohydrate source. Adult females were fed with defibrinated mutton blood (Biolife Italiana) using a Hemotek system. After mating, eggs were shipped to Radboud University

Nijmegen, the Netherlands, where adults (F2) were reared and transported to the BSL3 laboratory at Wageningen University, the Netherlands.

Aedes aegypti ir01115 or *Aedes aegypti* Kenya were offered infectious blood meals or were injected with ZIKV or ZIKV Δ SF1 as described in the main manuscript.

Construction of RNA-aptamer and protein expression plasmids

To identify RNA-protein interactions, aptamer constructs were designed based on the strategy of Leppek *et al.*, 2014 (2). The ZIKV sfRNA sequence was PCR amplified from pZIKV_{IC} using primers 7,8 containing a T7 promoter overhang and cloned into pJET1.2 to generate pJET-T7-sfRNA^{ZIKV}. pJET-T7-sfRNA^{ZIKV} was digested with PstI (NEB) and XbaI (NEB), which removes the original T7 promoter and a residual XbaI site, to generate pT7-ZIKV^{sfRNA}. Complementary oligos 9,10 containing the S1m-aptamer sequence were designed to generate compatible BamHI and BgIII overhangs. Oligos were annealed and ligated with T4 DNA ligase (Promega) in the presence of BamHI and BgIII to produce 1x-S1m, 2x-S1m and 4x-S1m DNA fragments that were subsequently ligated into pT7-sfRNA^{ZIKV} to generate pT7-S1m-sfRNA^{ZIKV}, pT7-2XS1m-sfRNA^{ZIKV} and pT7-4XS1m-sfRNA^{ZIKV}. Next, the WNV sfRNA and NS2A sequences were amplified with primers 11,12 and 13,14, respectively, from pWNV_{IC}. PCR products were cloned as NdeI/XbaI (NEB) fragments into pT7-4XS1m-sfRNA^{ZIKV} to replace the ZIKV sfRNA sequence and generate pT7-4XS1m-sfRNA^{WNV}, and pT7-4XS1m-NS2A.

To generate expression vectors of the characterized sfRNA-binding proteins, enhanced green fluorescent protein (EGFP) was PCR-amplified from pEGFP-N1 with primers 15,16 that introduce attB1/2, Ascl, EcoRI and NdeI sites and Gateway cloned (Invitrogen) into pDONR207 to generate pDONR-EGFP. Complementary oligos 17,18 containing the foot-and-mouth disease (FMDV) 2A ribosomal skipping element followed by a three-tandem repeat FLAG-tag (2A-3XFLAG) were annealed and ligated as Ascl/EcoRI (NEB) fragment into

pDONR-EGFP-3F. The genes coding for ME31B (AAEL008500), ATX2 (AAEL007805), LSM12 (AAEL007820) and 60sRp were PCR-amplified from Aag2 cells total RNA-derived cDNA using Q5 High-Fidelity DNA polymerase (NEB) and primers 19,20 (ME31B), 21,22 (ATX2), 23,24 (LSM12) or 25,26 (60sRp). PCR products were cloned as EcoRI/NdeI (ATX2, 60sRp, LSM12) or MfeI/NdeI(ME31B) fragment into pDONR-EGFP-3F and Gateway cloned into the previously described pPUB (Göertz et al., 2018) to generate pPUB-3F-ME31B, pPUB-3F-ATX2, pPUB-3F-LSM12 and pPUB-3F-60sRp. The ME31B PCR product was additionally cloned as MfeI/NdeI fragment into pDONR-EGFP and subsequently Gateway cloned into pPUB to generate pPUB-EGFP-ME31B.

JAK/STAT and Toll pathway stimulation

To characterize induction of the JAK/STAT and Toll pathway after virus infection, Aag2 cell monolayers were infected with ZIKV, ZIKV Δ SF1, WNV or WNV Δ SF1+2 at 40-50% confluence at an MOI of 1. The cells were incubated for 2 h, washed thrice with PBS and fresh culture medium was added. The cells were incubated at 28 °C until harvest. DH10 β *Escherichia coli* was grown overnight in 5 ml lysogeny broth and centrifuged for 5 min at 3,000 g. After washing twice with PBS, the pellet was resuspended in 500 μ l Schneider's medium supplemented with 10% FBS. The bacteria were heat-inactivated by 10 min incubation at 90 °C and the absorption at 600 nm was measured. An absorbance unit of 1 was considered equivalent to 1×10^9 bacteria per ml (Hernandez et al., 1994). The Aag2 cells were incubated in presence of 500 heat-inactivated bacteria per cell. Gene expression was measured by qRT-PCR at the indicated time-points.

***In vitro* RNA synthesis**

In vitro RNA was produced with either T7 or Sp6 RNA Polymerase (NEB) according to the manufacturer's protocols. To generate linear templates for production of S1m-aptamer containing RNAs, the corresponding plasmids were used as template for a PCR reaction with forward primer 27 and the corresponding reverse primer 28-30. Truncated sfRNA species

were generated by using forward primer 27 in combination with reverse primers 31-36. PCR products were gel-purified and additionally purified by phenol-chloroform-extracted before proceeding with T7 *in vitro* RNA synthesis. For generation of dsRNA for gene-silencing, partial gene sequences of ME31B, ATX2, AAEL018126 and Luciferase were amplified with primers 37-44, that introduce flanking T7 promoters. PCR products were purified by phenol-chloroform extraction and 1 µg DNA was used as template for *in vitro* RNA synthesis using T7 RNA polymerase.

XRN1-stalling assays

XRN1 stalling assays were used to investigate the formation of sfRNA after partial XRN1 degradation. Prior to XRN1 stalling assay, the RNA was renatured by incubation at 56 °C for 5 min, 2 min incubation at room temperature (RT) and stored on ice. *In vitro* XRN1 stalling assays were performed with Terminator 5' phosphate-dependent exonuclease (Epicentre) according to the manufacturer's protocol and the reaction was terminated by addition of 100 mM EDTA.

RNA electrophoreses & northern-blotting

Total RNA was size-separated by denaturing gel-electrophoresis in 6% polyacrylamide 7 M urea/TBE gel. Gels were stained with ethidium bromide and visualized with a Bio-Rad Gel Doc scanner. Northern-blotting and probe synthesis was performed as described previously (3). Briefly, RNA was semidry blotted onto a Hybond-N membrane (Amersham Biosciences), UV cross-linked and hybridized overnight with PCR-generated digoxigenin (DIG)-labelled probes in modified Church/10% formamide buffer at 50 °C. Blots were probed with alkaline-phosphatase (AP)-conjugated α-DIG antibodies (11093274910; Roche) and developed with nitroblue tetrazolium (NBT)-BCIP (5-bromo-4-chloro-3-indolylphosphate) solution (Roche) until sufficient signal was achieved. The DIG-labelled WNV 3'UTR specific-probe was described previously (3). The ZIKV 3'UTR specific DIG-labelled probe was generated by PCR with DIG-labelled nucleotides (Roche), primers 63,64 and pZIKV_{IC} as template.

RNA-affinity purification

RNA-affinity purification was based on the 4X S1m optimized streptavidin-binding RNA-aptamer system which has high affinity for streptavidin (2). For samples prepared for nano liquid chromatography-mass spectrometry (nano LC-MS/MS) all subsequent steps were performed in protein LoBind tubes (Eppendorf). For RNA-affinity purification with overexpressed proteins the protocol was downscaled. A 50% Streptavidin Sepharose High Performance bead-slurry (SA-beads; GE Healthcare) was equilibrated by washing thrice with SA-RNP lysis buffer (20 mM Tris-HCl (pH 7.5), 150 mM NaCl, 1.5 mM MgCl₂, 2 mM DTT, 2 mM vanadylribonucleosid complex RNase inhibitor (VRC; NEB)) supplemented with Halt Protease and Phosphatase inhibitor cocktail (ThermoFisher) for samples analysed by nano LC-MS/MS or Complete protease inhibitor cocktail (Roche) for samples analysed by western blot. Beads were washed by 1 min 240 g centrifugation at 4 °C followed by resuspension of the SA-beads. The final pellet of equilibrated SA-beads was resuspended 1:1 in SA-RNP lysis buffer. Per 100 µl equilibrated SA-beads 20 µl of DNase-treated *in vitro* transcribed 4XS1m aptamer-containing RNA was dissolved to a total volume of 50 µl in SA-RNP lysis buffer. RNA was renatured by incubation at 56 °C for 5 min, 37 °C for 10 min, and RT for 2 min, and stored on ice until further use. Five percent of the total volume was stored in TRIzol (Invitrogen) to analyse the quality of the input-RNA. To the remaining renatured RNA 100 µl equilibrated 50% SA-bead slurry was added and supplemented with 80 U RNasin (Promega). RNA and bead mixtures were incubated at 4 °C for 2.5 h with overhead rotation, with manual mixing every 15 mins to ensure homogeneous RNA to bead coupling. RNA-bound beads were collected by 2 min 110 g centrifugation at 4 °C. Five percent of the supernatant was stored in 500 µl TRIzol to analyse the quality of the unbound RNA. To prepare Aag2 cells lysates for RNA-affinity purification the culture medium of Aag2 cell monolayers was aspirated and the cells were washed once with PBS. Cells were detached by scraping, pelleted by 5 min 270 g centrifugation and washed twice with PBS. Aag2 cell pellets were lysed in SA-RNP lysis buffer supplemented with 1% NP-40 by 20 min incubation on ice. Nuclei were lysed by forcing the

lysates through a 0.8 × 0.4 mm needle and the cell debris was removed by 15 min 20,800 g centrifugation at 4 °C. Protein concentrations were determined by Bradford Protein Assay (Bio-Rad) following the manufacturer's protocol and absorption was measured using a FLUOstar Optima microplate reader (BMG Labtech). Cell lysates (2.7 – 3.0 mg protein) were pre-cleared by incubation with 25 µl Avidin agarose beads (Thermo Pierce) at 4 °C for 30 min under overhead rotation. Beads were removed by 1 min 20,800 g centrifugation at 4 °C and the supernatant was added to 50 µl 50% SA-beads and incubated for 2.5 h at 4 °C under overhead rotation. Beads were removed by 1 min 20,800 g centrifugation at 4 °C and the supernatant was added to a new tube and supplemented with 40 U RNasin. For protein-to-RNA coupling, 100 µl pre-cleared lysate was added to ~50 µl of RNA-bound SA-beads and incubated at 4 °C for 3.5 h under overhead rotation. Beads were collected by 1 min 110 g centrifugation at 4 °C and resuspended in SA-wash buffer (20 mM Tris-HCl (pH 7.5), 300 mM NaCl, 5 mM MgCl₂, 2 mM DTT) supplemented with VRC and protease inhibitors. A total of five wash steps were performed followed by a final wash with SA-wash buffer supplemented with only protease inhibitors. The final pellet was eluted by addition of 30 µl SA-elution buffer (20 mM Tris-HCl, 30 mM NaCl, 5 mM MgCl₂, 2 mM DTT) supplemented with protease inhibitors and 0.6 µg RNase A (Invitrogen) followed by 10 min incubation at 4 °C. Beads were removed by 1 min centrifugation at 3,800 g at 4 °C, ~30 µl eluate was collected and the residual beads were removed by 1 min centrifugation at 3,800 g at 4 °C. The final eluate was supplemented with 10 µl 4X SDS loading buffer (278 mM Tris-HCl, 18% glycerol, 4.5% SDS, 0.02% bromophenol blue, 10% β-mercapto-ethanol). Samples were stored at -20°C until further use.

Mass spectrometry

RNA-affinity purified proteins were size-separated shortly (1 cm) on a Mini-PROTEAN TGX Precast gel (Bio-Rad) by SDS-PAGE. Gels were stained for 1 h with Coomassie Brilliant Blue at RT and de-stained overnight with demineralized-water. Gels were washed thrice with demineralized-water and cysteine reduction was performed by incubation in 25 ml 10 mM DTT in 50 mM NH₄HCO₃ (pH 8.0) at 60 °C for 2 h. Alkylation was performed by incubation in 25 ml

20 mM C₂H₄INO in 0.1 M Tris/HCl (pH 8.0) at RT for 30 min under dark conditions. Each lane was cut into 1 mm² pieces and proteins were digested by overnight incubation with 250 ng Trypsin in a total volume of 75-150 µl 50 mM NH₄HCO₃ (pH 8.0) at RT. The pH was decreased to 3 by addition of trifluoroacetic acid and peptides were concentrated with in-house C18 µColumns. High-quality peptide identification was performed by nano LC-MS/MS using reversed phase nano LC (Proxeon) in combination with an LTQ - Orbitrap XL. The *Aedes aegypti* AaegL5.1 peptide sequences (4) (retrieved from Vectorbase on 24-04-2018) were used as a reference for peptide identification. Peptides were identified and quantified with MaxQuant as previously described (5, 6) and filtering was performed in Perseus to retrieve proteins with ≥ 2 peptide hits, of which ≥ 1 unique peptide(s). Nano LC-MS data analysis (false discovery rates were set to 0.01 on peptide and protein levels) and additional result filtering (minimally 2 peptides are necessary for protein identification of which at least one is unique and at least one is unmodified) were performed as described previously (7, 8). To analyse the relative abundance of proteins, their normalized label-free quantification (LFQ) intensities were compared (9). Nano LC-MSMS system quality was checked with PTXQC (10) using the MaxQuant result files.

Western blotting

Proteins were separated by SDS-PAGE and semi-dry blotted onto Immobilon-P membranes (Merck Millipore), blocked overnight at 4 °C with 1% milk powder (MP)/PBS-0.05%-Tween-20 (PBST) and probed for 1 h at RT with primary antibodies α-GFP (1:2000; A6455 Molecular Probes) or α-FLAG (1:2000; F3165 Sigma Aldrich) diluted in 1% MP/PBST. Membranes were washed thrice for 5 min with PBST and probed for 1 h at RT with AP-conjugated secondary antibody goat-α-rabbit-AP (1:2500; D0487 Dako) or goat-α-mouse-AP (1:2500; A5153 Sigma-Aldrich) diluted in PBST. Membranes were washed thrice for 5 min with PBST and developed with NBT/BCIP until the desired signal was reached.

Statistics & software

All statistical analyses were performed in IBM SPSS Statistics 23, unless stated otherwise. Titers of mosquito body and saliva samples were assessed for normality with Kolmogorov-Smirnov test. Data that did not follow a normal distribution was Log₁₀ transformed and re-assessed for normality. Normally distributed data was compared by unpaired two-tailed t-test ($\alpha=0.05$) and data that did not follow a normal distribution was analysed by Mann-Whitney U test ($\alpha=0.05$). Silencing efficiencies and relative gene expression as determined by qRT-PCR were compared by unpaired two-tailed t-test ($\alpha=0.05$). Gene expression of JAK/STAT and Toll-pathway regulated genes were compared by one-way ANOVA with Tukey's post-hoc test ($\alpha=0.05$). Viral titers and genome copies after silencing of sfRNA-binding candidates were compared by one-way ANOVA with Tukey's post-hoc test ($\alpha=0.05$). Infection, transmission and dissemination rates were compared by two-tailed Fisher's exact test ($\alpha=0.05$) using GraphPad Quickcalcs. Graphs were produced in GraphPad Prism 5. Protein interaction networks were produced on the STRING database V10.5 (11) using the closest orthologs in *Drosophila* listed on Vectorbase (12) with a minimum interaction score of 0.7. Asterisks in the manuscript figures indicate significance: * $P \leq 0.05$, ** $P \leq 0.01$, *** $P \leq 0.001$.

Supplemental References

1. Crochu S, et al. (2004) Sequences of flavivirus-related RNA viruses persist in DNA form integrated in the genome of *Aedes* spp. mosquitoes. *J Gen Virol* 85(7):1971–1980.
2. Leppek K, Stoecklin G (2014) An optimized streptavidin-binding RNA aptamer for purification of ribonucleoprotein complexes identifies novel ARE-binding proteins. *Nucleic Acids Res* 42(2):1–15.
3. Göertz GP, et al. (2016) Noncoding subgenomic Flavivirus RNA Is processed by the mosquito RNA interference machinery and determines West Nile virus transmission by *Culex pipiens* mosquitoes. *J Virol* 90(22):10145–10159.
4. Matthews BJ, et al. (2018) Improved reference genome of *Aedes aegypti* informs arbovirus vector control. *Nature* 563(7732):501–507.
5. Lu J, et al. (2011) Filter-aided sample preparation with dimethyl labeling to identify and quantify milk fat globule membrane proteins. *J Proteomics* 75(1):34–43.
6. Wendrich JR, Boeren S, Möller BK, Weijers D, De Rybel B (2017) In Vivo Identification of Plant Protein Complexes Using IP-MS/MS. *Plant Hormones: Methods and Protocols*, eds Kleine-Vehn J, Sauer M (Springer New York, New York, NY), pp 147–158.
7. Smaczniak C, et al. (2012) Proteomics-based identification of low-abundance signaling and regulatory protein complexes in native plant tissues. *Nat Protoc* 7(12):2144–2158.
8. Wendrich JR, Boeren S, Möller BK, Weijers D, De Rybel B (2017) In Vivo Identification of Plant Protein Complexes Using IP-MS/MS. *Plant Hormones: Methods and Protocols*, eds Kleine-Vehn J, Sauer M (Springer New York, New York, NY), pp 147–158.

9. Cox J, et al. (2014) Accurate Proteome-wide Label-free Quantification by Delayed Normalization and Maximal Peptide Ratio Extraction, Termed MaxLFQ. *Mol Cell Proteomics* 13(9):2513–2526.
10. Bielow C, Mastrobuoni G, Kempa S (2016) Proteomics Quality Control: Quality Control Software for MaxQuant Results. *J Proteome Res* 15(3):777–787.
11. Szklarczyk D, et al. (2015) STRING v10: protein-protein interaction networks, integrated over the tree of life. *Nucleic Acids Res* 43(Database issue):447–452.
12. Giraldo-Calderon GI, et al. (2015) VectorBase: an updated bioinformatics resource for invertebrate vectors and other organisms related with human diseases. *Nucleic Acids Res* 43:707–713.
13. Göertz GP, Abbo SR, Fros JJ, Pijlman GP (2017) Functional RNA during Zika virus infection. *Virus Res* 254:1–13.

Supplemental Figure Legends

Fig. S1: A ZIKV-mutant defective in sfRNA1 production is not attenuated in Aag2 cells.

(A) Left: schematic overview of the ZIKV sfRNA secondary structure and the production of sfRNA1 and sfRNA2 by stalling of the exoribonuclease XRN1/Pacman. SL stem loop; DB dumbbell; UTR untranslated region, adapted from (13). Right: schematic overview of the introduced mutations in SL-I and SL-II of the ZIKV 3'UTR to generate ZIKV Δ SF1 and ZIKV Δ SF1+2. Numbers indicate the nucleotide position in the 3'UTR of the start position of sfRNA1 and sfRNA2. Black lines indicate pseudoknot interactions. Mutated nucleotides in ZIKV Δ SF1 and ZIKV Δ SF1+2 are shaded. **(B)** Northern blot using a 3'UTR-specific probe on total RNA from ZIKV or ZIKV Δ SF1 infected C6/36, Aag2, AP-61 and U4.4 cells. **(C)** Aag2 cells were infected with ZIKV or ZIKV Δ SF1 at a multiplicity of infection (MOI) of 5 and the titer in the supernatant was determined at 24 and 48 hours post infection (hpi) by end-point dilution assay (EPDA) on Vero cells. Shown are the mean viral titers \pm standard error of the mean from duplicate replicates. Dotted line indicates the EPDA detection limit.

Fig. S2: ZIKV sfRNA determines virus accumulation in the saliva of recently colonized *Aedes aegypti* mosquitoes from French Guiana and Kenya. **(A)** Female *Ae. aegypti* (French Guiana ir0115 and Kenya) were fed with an infectious blood meal containing 3.0 \times 10⁶ TCID₅₀/ml ZIKV or ZIKV Δ SF1. Engorged females were incubated for 14 days at 28 °C and infection and transmission rates were determined by infectivity assay on Vero cells. **(B)** Female *Ae. aegypti* (French Guiana ir0115 and Kenya) were intrathoracically injected with ~400 TCID₅₀ of ZIKV or ZIKV Δ SF1. The mosquitoes were incubated for 7 days at 28 °C and infection and transmission rates were determined by infectivity assay on Vero cells. Statistics were performed by Fisher's exact test. **(C)** Viral titers in the bodies of virus-positive bodies and saliva samples were determined by EPDA. Shown are the median titers and statistics were

performed by Mann-Whitney U-test. Dotted lines indicate the EPDA detection limit. * $P \leq 0.05$,

** $P \leq 0.01$, *** $P \leq 0.001$, ns, not-significant.

Fig. S3: SfRNA does not modulate the expression of Toll and JAK/STAT regulated genes early after infection of *Ae. aegypti* cells. Aag2 cells were infected with (A-D) ZIKV, ZIKV Δ SF1, (E-H) WNV, WNV Δ SF1+2, at a multiplicity of infection of 1, treated with heat-inactivated bacteria (+) or left untreated (mock). At 24 hours post treatment, total RNA was extracted and subjected to qRT-PCR to quantify the expression of the Toll-regulated genes (B,F) CecG and (C,G) DefC, the JAK/STAT regulated gene (D,H) TEP22 and the copies of (A,E) viral genomic (vg)RNA. Gene expression was normalized to the rpS7 reference gene and the untreated mock control. Shown is the mean normalized relative expression of two replicates from three independent biological experiments \pm standard error of the mean. Statistics were performed by One-way ANOVA with Tukey's post-hoc test. Cq, cycle of quantification; ns, not significant. ** $P \leq 0.01$, *** $P \leq 0.001$, ns, not-significant.

Fig. S4 Small RNA sequencing of ZIKV and ZIKV Δ SF1-infected *Ae. aegypti*. Small RNAs were sequenced at 14 days post-exposure from three pools of 5-6 full-disseminated *Ae. aegypti* mosquitoes infected with ZIKV or ZIKV Δ SF1 via either a blood meal (A, C, E) or intrathoracic injections (B, D, F). **(A-B)** Size distributions of small RNAs that mapped to the ZIKV genome. Small RNA reads were normalized as percentage of reads from the total number of reads in the library. **(C-F)** Small RNA reads from one representative pool of blood fed and one pool of injected mosquitoes with a length of 21 nts were mapped along the (+) strand (C & D) and (-) strand (E & F) of the ZIKV genome. Insets show reads that mapped specifically to the ZIKV 3'UTR. Reads from ZIKV-infected mosquitoes are shown in black, reads from the ZIKV Δ SF1-infected mosquitoes are shown in grey.

Fig. S5 Ae. aegypti does not produce bona fide viral PIWI-interacting (pi)RNAs to ZIKV infection. Sequence logos of sense (+) and antisense (-) 25-30 nt small RNAs that map to the ZIKV or ZIKV Δ SF1 genome, and the probability of overlap length after an infectious blood meal and intrathoracic injections.

Fig. S6 A streptavidin-binding aptamer approach to detect sfRNA binding proteins. (A) Left: schematic overview of the constructs used to produce 4XS1m-aptamer-fused ZIKV sfRNA, WNV sfRNA and the control RNA. Right: Schematic experimental overview. 4XS1m-aptamer bound RNAs are bound to streptavidin beads and used to purify *Ae. aegypti* proteins with affinity for the bait RNA. RNA-bound proteins were eluted by RNase A digestion of the bait RNA and identified and quantified by mass spectrometry. **(B)** Streptavidin beads were incubated with *in vitro* transcribed RNA of 4XS1m-ZIKV-sfRNA, 2XS1m-ZIKV-sfRNA, ZIKV-sfRNA, 4XS1m-WNV-sfRNA or 4XS1m-control. RNA was extracted from input (I), unbound (U) and bound (B) RNA and analysed on TBE/poly-acrylamide gel. **(C)** *In vitro* transcribed RNA of 4XS1m-ZIKV-sfRNA, 2XS1m-ZIKV-sfRNA, ZIKV-sfRNA, 4XS1m-WNV-sfRNA or 4XS1m-control was treated with 0, 0.1 or 1 unit (U) of *in vitro* exoribonuclease (XRN1) and analysed on TBE/poly-acrylamide gel.

Fig. S7 ZIKV and WNV sfRNA interact with two distinct *Ae. aegypti* protein networks. Protein interaction network prediction of proteins that were ≥ 3 -fold enriched in both the ZIKV and WNV sfRNA samples using the STRING database using high confidence level (≥ 0.7) based on their *Drosophila* orthologs. The thickness of the lines correlates with the confidence of the interaction.

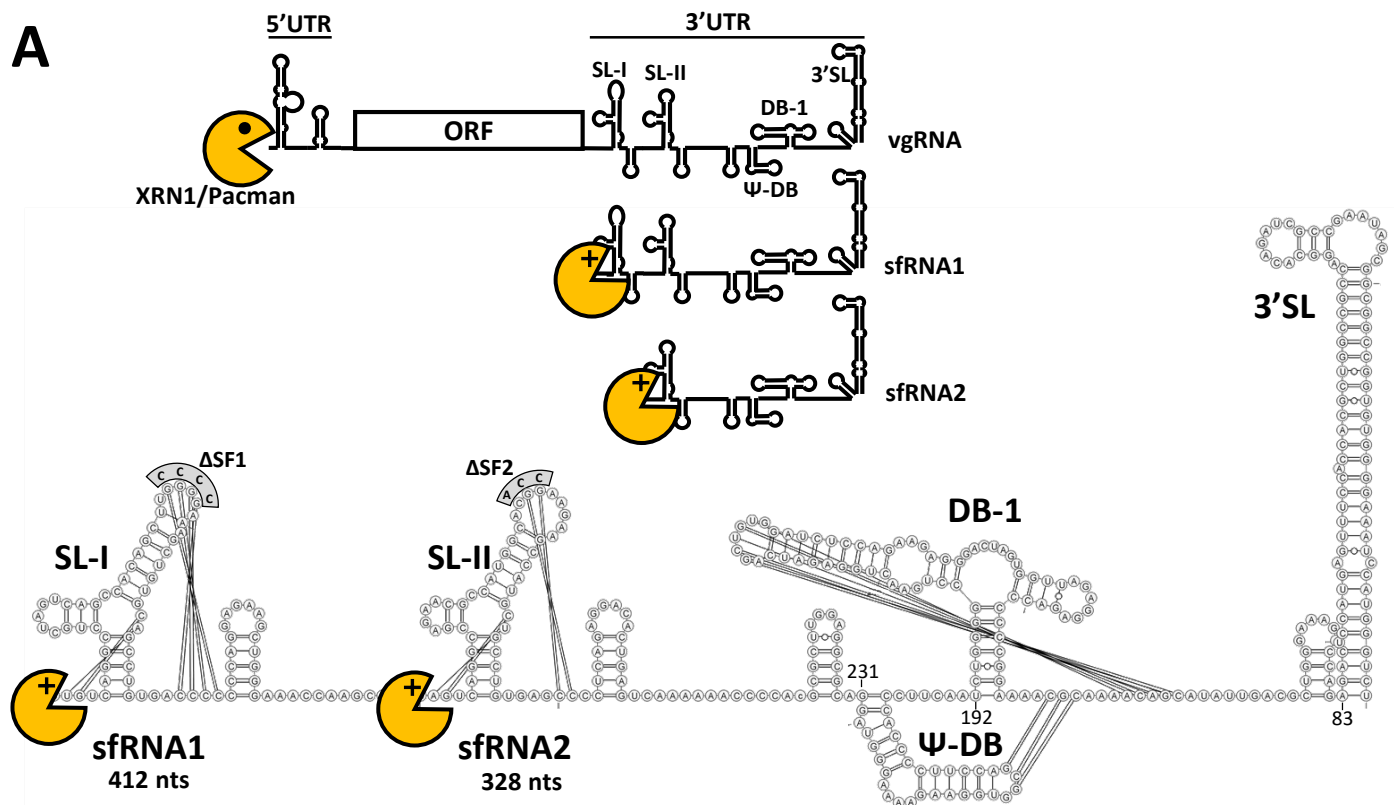
Fig. S8 ATX2 interacts with ZIKV and WNV sfRNA indirectly via ME31B. ME31B was expressed fused N-terminally to EGFP (ME31B-EGFP) and ATX2 was expressed N-terminally fused to EGFP followed by a foot-and-mouth disease virus 2A ribosome skipping sequence and a triple FLAG (3F)-tag (3F-ATX2). Lysates of Aag2 cells transfected with pPUB-3F-ATX2, pPUB-EGFP-ME31B or both pPUB-3F-ATX2 and pPUB-EGFP-ME31B were prepared.

Lysates were subjected to RNA-affinity purification and RNA-bound proteins were detected by western blot with α -Flag and α -GFP antibodies.

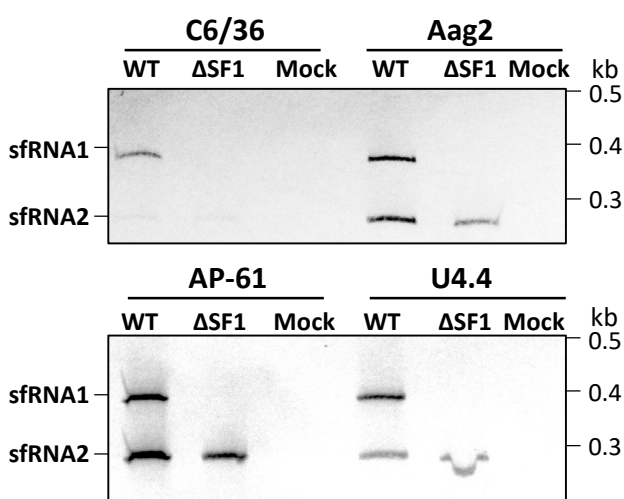
Fig. S9 Confirmation of silencing efficiencies by qRT-PCR. Aag2 cells were transfected with dsRNA against Luciferase (Luc), ME31B, Ataxin-2 (ATX2) or AAEL018126 (AAEL) and re-transfected after 48 hours. RNA was harvested and subjected to qRT-PCR with gene-specific primers, normalized to the rpS7 reference gene and the relative gene expression was computed compared to the dsLuc transfected control. Unpaired t-tests were used to compare silencing efficiencies. ** $P \leq 0.01$, *** $P \leq 0.001$

Figure S1

A



B



C

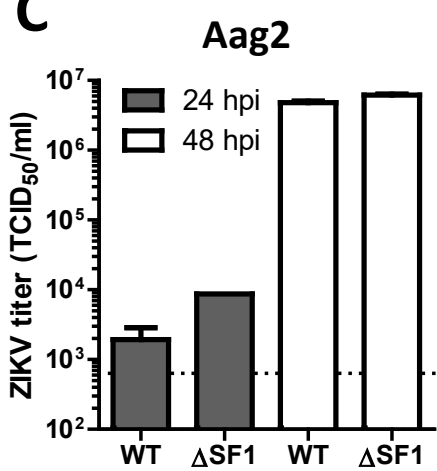


Figure S2

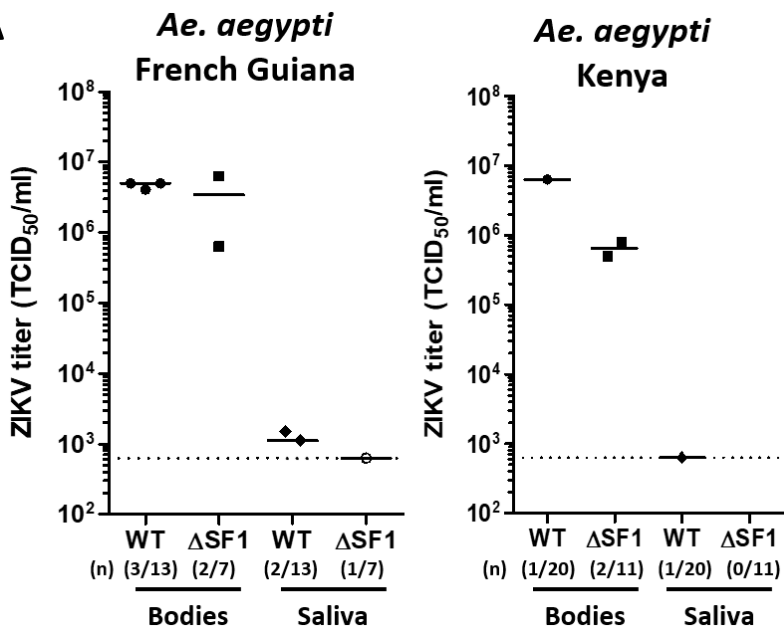
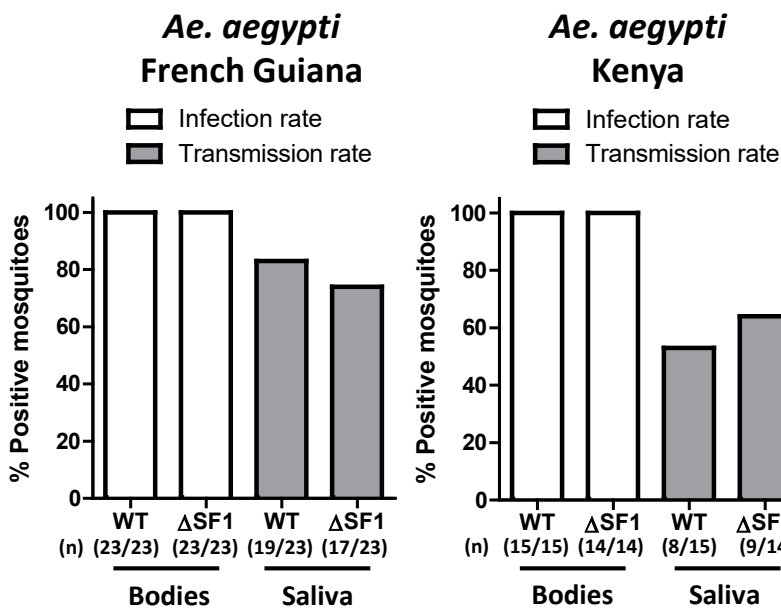
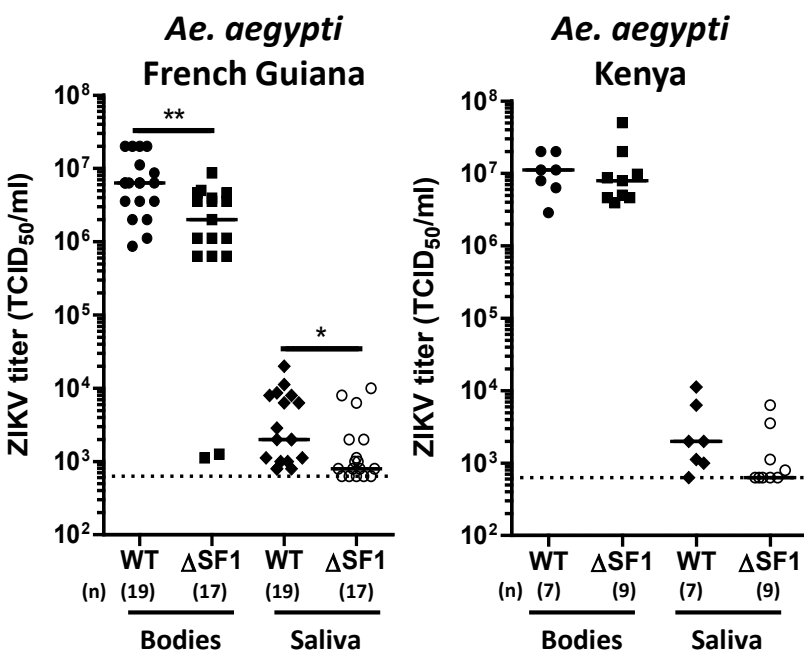
A**B****C**

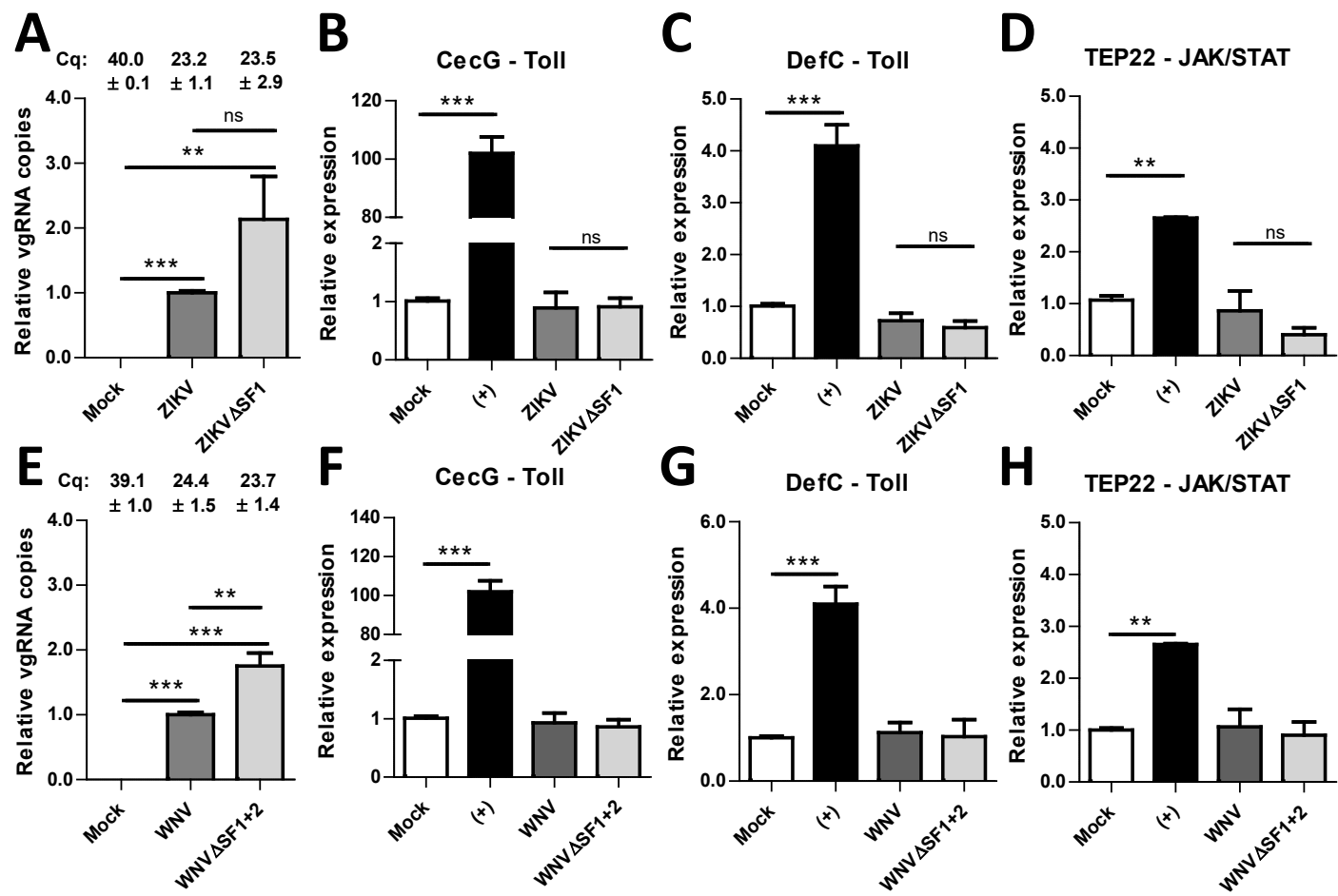
Figure S3

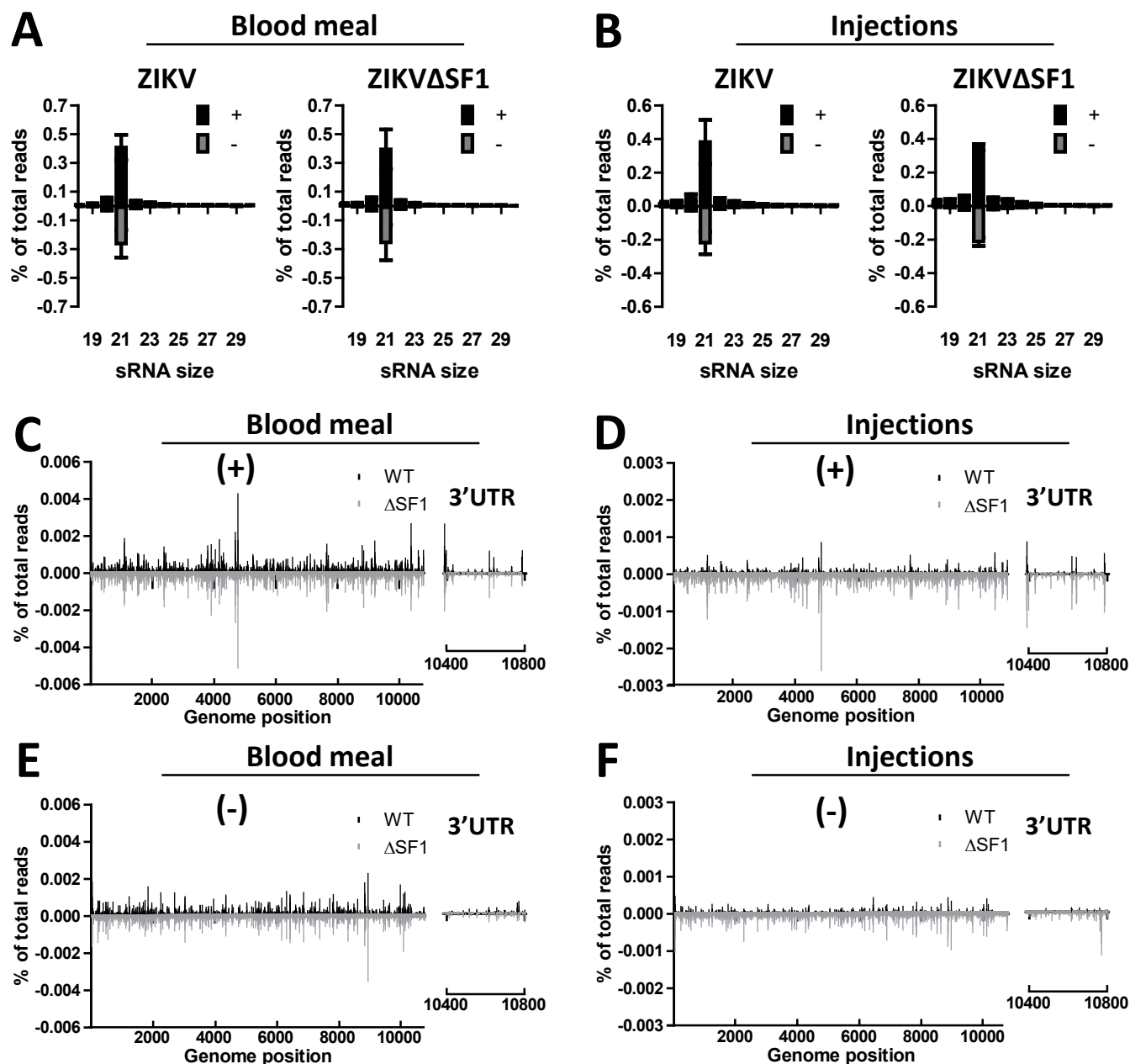
Figure S4

Figure S5

Bloodmeal Injection

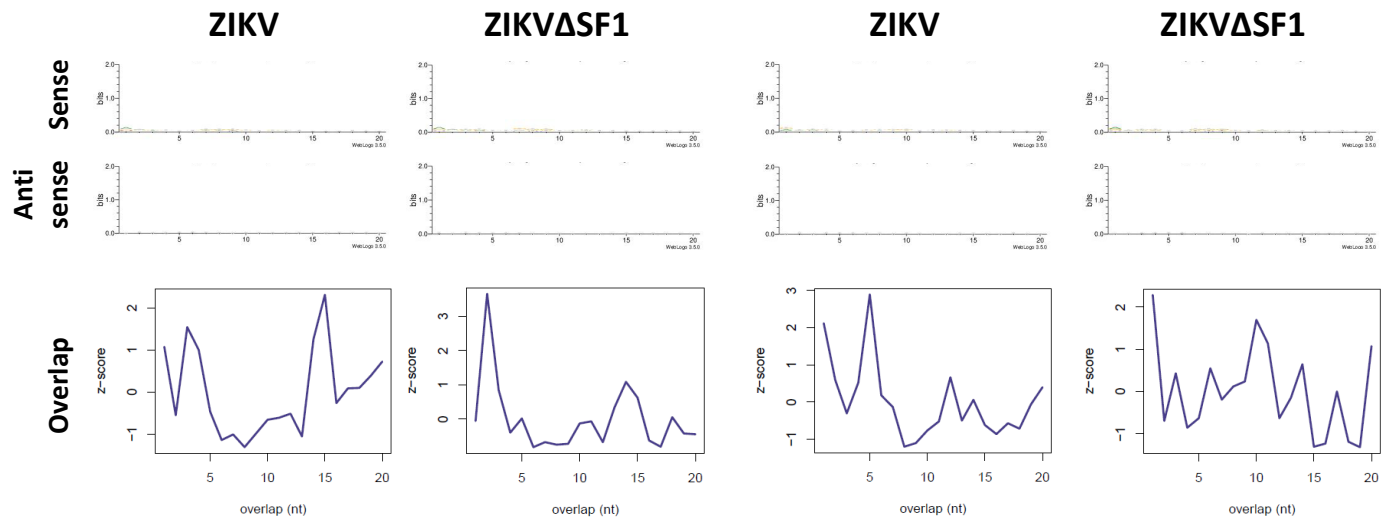


Figure S6

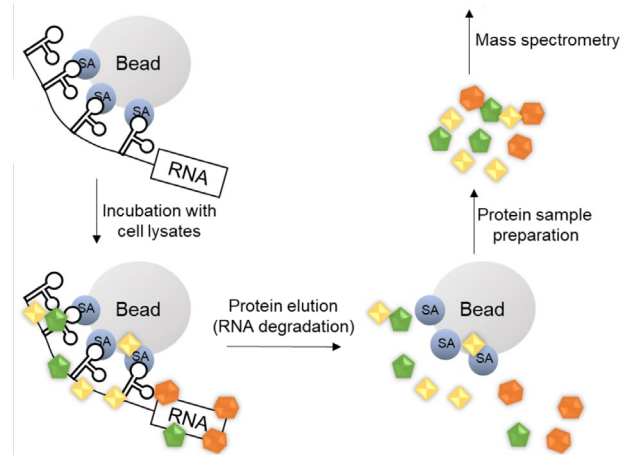
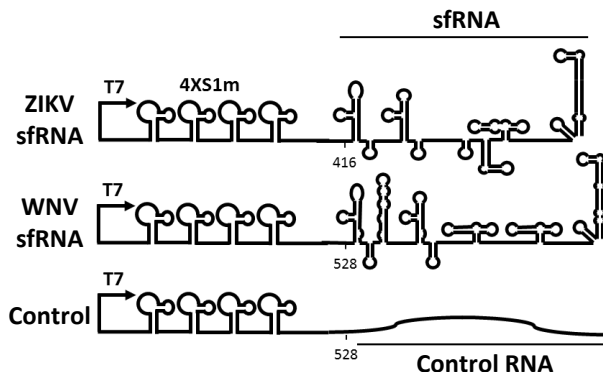
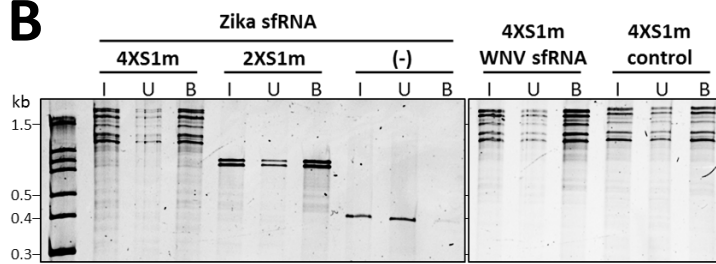
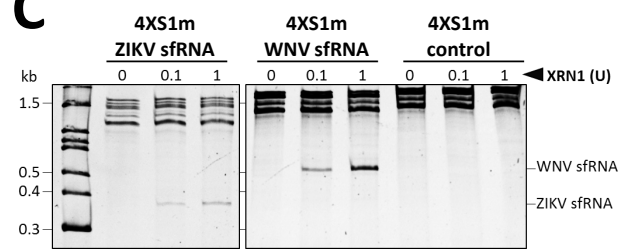
A**B****C**

Figure S7

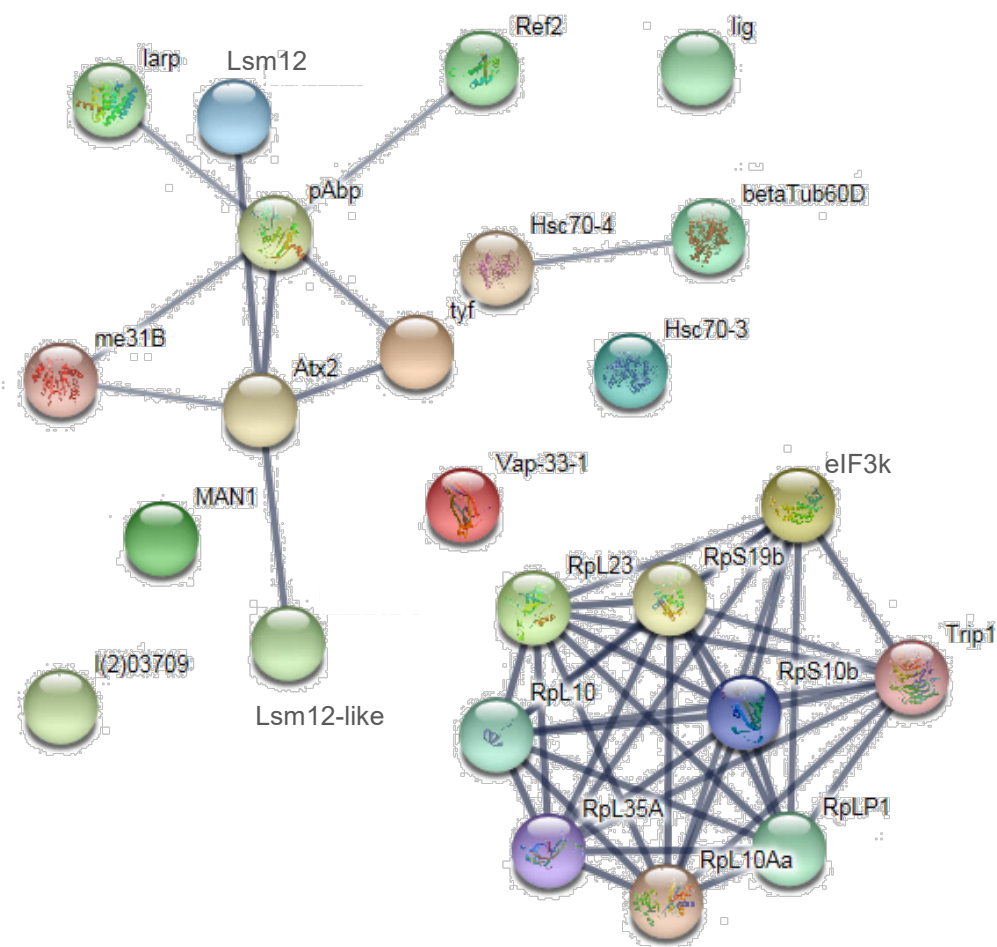


Figure S8

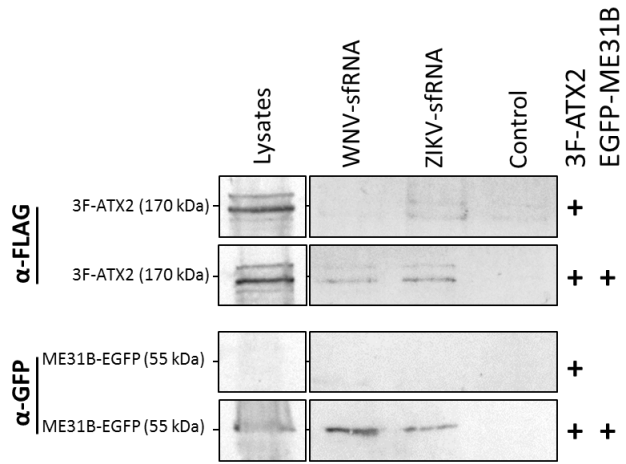


Figure S9

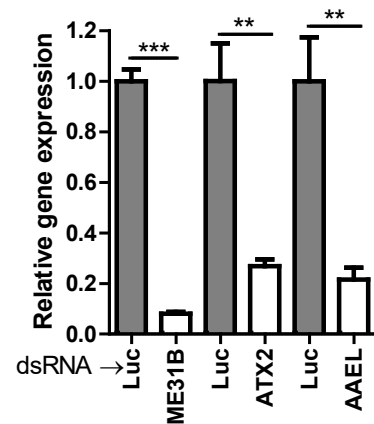


Table S1: Primers used in this study

#	Primer	Sequence (5'→3')
1	SubZika-F	GGCTAGATTCTAGAGTTCGAAGCCCTTG
2	SubZika-R	GGCCAAGTTTCCGCGAGGTATC
3	Zika-PK1-F	GCCACAGCTTCCCCAAAGCTGTGCAGCCTGTGA
4	Zika-PK1-R	GCACAGCTTGGGAAGCTGTGGCTGACTAGCA
5	Zika-PK2-F	CGCCATGGCAACCAAGAACGCCATGCTGCCTGT
6	Zika-PK2-R	ATGGCTTCTGGTGCATGGCGTTCTCGGC
7	T7-ZIKV sfRNA-F	GGCTGCAGTAATACGACTCACTATAAGGGAGAGGTACCGGAT CCCATATGATGTTGTCAGGCCTGCTAGTCAGC
8	T7-ZIKV sfRNA-R	GGGAGCTCTCGGAATTCTAATCTCTAGAGACCCATG GATTCCCCACACC
9	S1m-F	/5PHOS/GATCCGTAGAAAATGCGGCCGCCGACCAGAAT CATGCAAGTGCCTAAGATAGTCGCGGTCGGCGGCC CATCTGCTGGGA
10	S1m-R	/5PHOS/GATCTCCCAGCAGATGCGGCCGCCGACCCGC GAATCTTACGCACCTGCATGATTCTGGTCGGCGGCC GCATTTCTACG
11	WNV-sfRNA-F	GGCATATGATGGAAGTCAGGCCAGATTAATGCTGC
12	WNV-sfRNA-R	GGGAATTCTAATCTCTAGAGATCCTGTGTTCTAGCACC ACC
13	WNV-NS2A-F	GGCATATGTACAACGCCGACATGATTGATCCTTTCA
14	WNV-NS2A-R	GGGAATTCTAATCTCTAGACTGTACACATCAAGGTTAG GCATTTAGTCCA
15	attB1-EGFP-F	GGGGACAAGTTGTACAAGAAAAAGCAGGCTTAATTAAA CCATGGTGAGCAAGGGCGAGGAG
16	attB2-EGFP-R	GGGGACCACTTGTACAAGAAAGCTGGGTACATATGGA ATTGGCGCGCCACTGTACAGCTCGTCCATGCCGA
17	2A-3XFLAG-F	CGCGCCAACTTGACCTGCTCAAGTTGCCGGCGACG TCGAGTCCAACCCAGGGCCGACTACAAAGACCATGA CGGTGATTATAAGATCATGACATCGATTACAAGGATG ACGATGACAAGG
18	2A-3XFLAG-R	AATTCTTGTACCGTCATCCTGTAATCGATGTCATGA TCTTTATAATCACCGTCATGGTCTTGTAGTCGGGCCCT GGGTTGGACTCGACGTCGCCGCCAACTTGAGCAGGT CAAAGTTGG
19	ME31B-F	CAATTGATGATGACTGAAACGCTGAATTCTAATAATCAT CTCAG
20	ME31B-R	CATATGTTATTGCTAATGTTCTGTTCTGTGTGC
21	ATX2-F	GGTGGGAATTCATGCATGCGGCTACATCACA
22	ATX2-R	GGTGGCATATGCTACTGAGCGGATGGATGCT
23	LSM12-F	GAATTCATGGCTGGTAGTTCAAGGATTGTTCTATT GG
24	LSM12-R	CATATGCTATTGGCAGAAACTGTTGCGGATGG
25	60sRp-F	GGTGGGAATTCATGGTAGGGAGGGACAAAGCTA
26	60sRp-R	GGTGGCATATGTTAATCGAACAGACCGAAGCCC
27	T7-F	TAATACGACTCACTATAAGGGAGAGGTACCGG
28	NS2A-RNA-R	CTGTACACATCAAGGTTAGGCATTTAGTCCA

29	WNV-sfRNA-RNA-R	AGATCCTGTGTTCTAGCACCAACCAG
30	ZIKV-sfRNA-RNA-R	AGACCCATGGATTCCCCACACC
31	ZIKV SL-II-R	TTTTTGACTCAGTGCCTCTGAGGGG
32	ZIKV ΨDB-R	GAAGGGTGGGAAGGTCGC
33	ZIKV DB2-R	AATATGCTGTTGCGTTTCCGGGG
34	WNV SL-IV-R	TTAACCCAGTCCACCTGGGG
35	WNV DB1-R	TTTTGACGCCGGTCTCCTCTAACC
36	WNV DB2-R	GTCAAATATGCTGTTCTTTGGTGTGTTGGCAC
37	dsME31B-F	TAATACGACTCACTATAGGGAGACCCTGGCGAGGGC TAAAAATGGT
38	dsME31B-R	TAATACGACTCACTATAGGGAGACCACAGTTCTTCACG CTCAGTGGG
39	dsATX2-F	TAATACGACTCACTATAGGGAGACCACCAAGGTGCC CCGAAAAAG
40	dsATX2-R	TAATACGACTCACTATAGGGAGACCACAAGTGCTGGTG ATGGATGGG
41	dsAAEL018126-F	TAATACGACTCACTATAGGGAGACCACCTCTCGCAAAA CTGGCAACG
42	dsAAEL018126-R	TAATACGACTCACTATAGGGAGACCACCTCTCCCATGT CGATGACGG
43	dsLuc-F	GTAATACGACTCACTATAGGGACTTACGCTGAGTACTTC
44	dsLuc-R	GTAATACGACTCACTATAGGGAAATCCCTGGTAATCCG
45	qPCR-rpS7-F	ATGGTTTCGGATCAAAGGT
46	qPCR-rpS7-R	CGATAGCCTCTTGCTGTTG
47	qPCR-CecG-F	GAAGCAGGTGGCCTCAAGAA
48	qPCR-CecG-R	TTAGCCCCAGCTACAAACAGG
49	qPCR-DefC-F	CTGCTCGTCACTCCTCCATC
50	qPCR-DefC-R	GCAC TGAGG CAAAG AGCAAC
51	qPCR-TEP22-F	AACGTGGCCTTGCCAATTG
52	qPCR-TEP22-R	CACTACCACCGTCGTTGACA
53	qPCR-ZIKV-F	GAGACGAGATGCGGTACAGG
54	qPCR-ZIKV-R	CGACCGTCAGTTGAACCTCA
55	qPCR-WNV-F	TGCACTCCTAGTCCTAGTGTGTTGGG
56	qPCR-WNV-R	TCTTGAATGTAGCCATGAGTGCC
57	qPCR-ME31B-F	CCCGAAAATGGCAGAGACCT
58	qPCR-ME31B-R	TCCTCTGGTCGAGGCACATA
59	qPCR-ATX2-F	ATGCAAACGATGGCAAACCC
60	qPCR-ATX2-R	GTTGGTTGGGTGAGGTGTGA
61	qPCR-AAEL018126-F	GGCAACGATACCGATTGTGC
62	qPCR-AAEL018126-R	GCTACTACTGGGCACGGTTT
63	ZIKV-probe-F	AGTCGCTACTTGGGTGAAGAAGGG
64	ZIKV-probe-R	GGAAACTCATGGAGTCTGGTCTTCC

Table S2. Mass Spec data ZIKV

Name (some based on orthology with <i>Drosophila</i>)	Gene IDs	Log difference	-log(p-value)	Log LFQ (protein abundance)								Proteins (#)	Peptides (#)	Unique peptides (#)	Mw (kDa)	
				ZIKV-sfRNA 1	ZIKV-sfRNA 2	ZIKV-sfRNA 3	NS2A 1	NS2A 2	NS2A 3	Proteins (#)	Peptides (#)					
Me31b	AAEL008500	2,534	2,809	7,643	7,474	7,011	5,098	4,300	5,128	2	28	28	50,4			
Ataxin-2	AAEL007805	2,227	2,264	6,831	6,357	7,301	5,208	4,300	4,300	6	11	11	104,2			
Protein lingerer	AAEL009607	1,515	0,924	6,372	6,774	4,300	4,300	4,300	4,300	16	4	4	127,4			
AAEL018126	AAEL018126	1,318	3,291	5,532	5,451	5,871	4,300	4,300	4,300	14	6	6	177,1			
Lsm12	AAEL007820	1,075	0,934	4,300	5,952	5,874	4,300	4,300	4,300	1	2	2	20,6			
AAEL024098	AAEL024098	1,039	0,745	6,233	6,155	6,900	5,526	4,300	6,346	1	9	9	68,3			
Nup358	AAEL020592	0,880	1,009	5,390	5,784	5,547	5,482	4,300	4,300	4	7	7	292,2			
Rp519	AAEL010756	0,811	0,319	6,539	6,621	4,300	6,428	4,300	4,300	3	9	9	17,3			
Rpl10a	AAEL013221	0,763	0,032	6,507	7,291	6,842	6,771	4,300	7,279	2	8	8	24,6			
eIF3i	AAEL013144	0,718	0,935	5,375	5,379	4,300	4,300	4,300	4,300	1	4	4	36,0			
Rpl23	AAEL015006	0,707	0,427	4,300	6,420	4,300	4,300	4,300	4,300	1	5	5	14,9			
Prohibitin	AAEL013952	0,677	0,432	6,200	6,586	5,817	5,857	4,300	6,415	4	8	8	39,0			
Rp510	AAEL002047	0,673	0,427	4,300	6,319	4,300	4,300	4,300	4,300	1	4	4	18,0			
Heat shock cognate 70	AAEL019403	0,653	0,334	6,383	6,834	6,244	6,893	4,300	6,309	3	18	14	71,1			
RNA and export factor binding protein 2	AAEL026243	0,631	0,427	4,300	6,194	4,300	4,300	4,300	4,300	1	3	3	27,3			
Tubulin	AAEL002848	0,617	0,346	6,414	6,644	5,805	6,148	4,300	6,566	1	14	5	50,8			
RplP1	AAEL005027	0,589	0,427	4,300	6,068	4,300	4,300	4,300	4,300	5	4	4	11,5			
eIF3-S5	AAEL009101	0,588	0,427	4,300	6,063	4,300	4,300	4,300	4,300	1	3	3	31,7			
La related protein	AAEL009070	0,586	0,418	5,785	5,658	4,300	5,385	4,300	4,300	3	5	5	169,5			
SAV_STRAV	AAEL006115	0,578	0,244	7,551	8,836	7,534	8,200	5,700	8,265	1	4	4	18,8			
eIF3k	AAEL006115	0,578	0,427	4,300	6,033	4,300	4,300	4,300	4,300	1	2	2	25,8			
Rpl35	AAEL008023	0,569	0,280	6,053	5,996	4,300	6,042	4,300	4,300	1	4	4	18,9			
Piwi5	AAEL013233	0,561	0,512	5,635	5,785	5,907	5,455	4,300	5,887	1	7	7	105,7			
PABP	AAEL010318	0,535	1,229	7,134	7,105	6,552	6,474	6,241	6,470	2	27	27	69,7			
Rpl10	AAEL025362	0,529	0,223	6,755	7,035	5,637	6,729	4,300	6,808	2	6	6	25,4			
Hsc70-3	AAEL026215	0,517	0,413	5,618	6,161	5,563	5,956	4,300	5,535	10	12	10	72,3			
Vap33	AAEL024800	0,512	0,427	4,300	5,836	4,300	4,300	4,300	4,300	2	2	2	31,1			
protein disulfide-isomerase A6 precursor	AAEL010065	0,508	0,304	5,653	5,876	4,300	5,706	4,300	4,300	3	7	7	47,7			
cathepsin l	AAEL002833	0,497	0,263	6,016	5,699	4,300	5,923	4,300	4,300	1	4	4	38,0			
Otefin	AAEL015180	0,493	0,427	4,300	5,778	4,300	4,300	4,300	4,300	1	4	4	45,6			
arginyl-tRNA synthetase	AAEL000199	0,473	0,427	4,300	5,719	4,300	4,300	4,300	4,300	1	7	7	75,6			
ATP synthase alpha	AAEL024040	0,473	0,369	4,989	5,875	4,300	4,300	4,300	5,146	2	2	2	27,0			
chaperonin-60kD	AAEL012175	0,453	0,229	5,868	6,838	5,636	6,275	4,300	6,409	1	13	13	59,4			
cotamer	AAEL013098	0,448	0,285	6,100	5,659	5,152	6,258	4,300	5,008	1	11	11	60,8			
Eukaryotic translation initiation factor 3 subunit H	AAFL007945	0,435	0,276	6,019	5,820	4,300	5,178	4,300	5,356	1	4	3	38,5			
proliferation-associated 2g4	AAEL012312	0,434	0,221	5,922	5,701	4,300	6,020	4,300	4,300	1	8	8	48,0			
Rpl38	AAEL027560	0,419	0,925	4,980	4,876	4,300	4,300	4,300	4,300	1	2	2	41,7			
cdk1	AAEL008621	0,414	0,427	4,300	5,543	4,300	4,300	4,300	4,300	3	2	2	34,6			
calponin/transgelin	AAEL006922	0,414	0,218	5,985	5,496	4,300	5,938	4,300	4,300	1	3	3	20,7			
tubulin alpha chain	AAEL013229	0,411	0,199	5,712	6,910	5,334	6,144	4,300	6,280	4	11	11	49,9			
Rpl38	AAEL005451	0,408	0,427	4,300	5,523	4,300	4,300	4,300	4,300	1	3	3	8,3			
Glyceraldehyde-3-phosphate dehydrogenase	AAEL016984	0,383	0,165	6,496	6,584	5,872	7,109	4,300	6,394	1	8	8	35,4			
AAEL019669	0,379	0,260	5,555	5,445	4,300	4,300	4,300	5,563	1	5	5	39,6				
AAEL008601	0,373	0,427	4,300	5,418	4,300	4,300	4,300	4,300	1	2	2	32,3				
translational activator gcn1	AAEL006187	0,366	0,427	4,300	5,398	4,300	4,300	4,300	4,300	1	3	3	293,3			
elongation factor 1 gamma	AAEL011288	0,365	0,203	6,435	5,925	5,320	6,106	4,300	6,179	1	12	12	48,9			
AAEL008171	0,360	0,185	5,164	6,100	4,300	5,885	4,300	4,300	2	11	11	96,4				
fuse-binding protein-interacting repressor serine/threonine protein kinase	AAEL004415	0,355	0,427	4,300	5,365	4,300	4,300	4,300	4,300	5	5	5	64,1			
AAEL000217	0,352	0,427	4,300	5,357	4,300	4,300	4,300	4,300	3	4	4	109,7				
Histone H4	AAEL028138	0,348	0,196	5,520	6,286	4,300	5,489	4,300	5,272	4	15	15	214,4			
CTP synthase	AAEL005455	0,340	0,427	4,300	5,186	5,835	5,008	5,361	4,300	5,323	101	3	3	11,4		
DEAD box ATP-dependent RNA helicase	AAEL010402	0,337	0,181	5,839	6,197	4,300	5,528	4,300	5,497	5	7	6	80,1			
Prohibitin	AAEL009345	0,335	0,151	6,089	6,456	4,300	5,694	4,300	5,846	1	8	8	29,9			
AAEL004978	0,332	0,344	5,127	5,258	4,300	5,090	4,300	4,300	2	3	2	68,7				
cytochrome B5	AAEL010017	0,331	0,427	4,300	5,292	4,300	4,300	4,300	4,300	1	2	2	14,7			
AAEL009169	0,328	0,427	4,300	5,285	4,300	4,300	4,300	4,300	12	2	2	93,1				
ebna2 binding protein P100	AAEL000293	0,322	0,237	5,369	5,384	4,300	5,487	4,300	4,300	1	4	4	103,4			
Pep12p	AAEL009398	0,319	0,427	4,300	5,256	4,300	4,300	4,300	4,300	1	3	3	33,9			
AAEL008741	0,317	0,193	5,494	5,514	4,300	5,756	4,300	4,300	1	7	7	109,6				
AAEL025547	0,312	0,427	4,300	5,235	4,300	4,300	4,300	4,300	1	3	3	93,3				
AAEL012904	0,312	0,122	5,770	6,043	4,300	6,578	4,300	4,300	1	8	8	49,9				
AAEL0024500	0,311	0,427	4,300	5,234	4,300	4,300	4,300	4,300	1	3	3	35,0				
rab6	AAEL006091	0,311	0,427	4,300	5,234	4,300	4,300	4,300	4,300	3	2	2	23,5			
Chaperonin	AAEL019990	0,310	0,427	4,300	5,230	4,300	4,300	4,300	4,300	5	2	2	54,3			
AAEL007765	0,304	0,182	5,497	5,499	4,300	5,785	4,300	4,300	7	4	4	42,4				
AAEL007650	0,303	0,262	5,240	5,269	4,300	5,301	4,300	4,300	1	4	4	57,9				
AAEL012746	0,299	0,173	5,229	5,759	4,300	5,790	4,300	4,300	1	9	9	59,5				
AAEL023188	0,298	0,427	4,300	5,193	4,300	4,300	4,300	4,300	1	3	3	68,1				
AAEL009041	0,291	0,427	4,300	5,174	4,300	4,300	4,300	4,300	3	2	2	19,7				
AAEL009123	0,287	0,427	4,300	5,162	4,300	4,300	4,300	4,300	1	4	4	56,2				
AAEL010467	0,286	0,203	5,695	5,598	4,300	5,177	4,300	5,257	1	5	5	39,8				
AAEL008738	0,282	0,118	6,073	5,549	4,300	5,743	4,300	6,032	1	13	10	98,9				
AAEL023552	0,280	0,150	4,300	5,955	5,885	4,300	5,193	4,300	5,807	4	3	3	35,7			
AAEL013675	0,278	0,131	4,300	6,326	4,300											

	AAEL003750	0.190	0.079	5,478	5,814	4,300	6,422	4,300	4,300	1	4	4	19,4
	AAEL021422	0.189	0.427	4,300	4,866	4,300	4,300	4,300	4,300	2	3	3	21,2
	AAEL006474	0.187	0.427	4,300	4,860	4,300	4,300	4,300	4,300	2	3	3	107,8
	AAEL019778	0.186	0.100	4,300	5,966	4,300	5,409	4,300	4,300	1	4	4	23,2
	AAEL007915	0.173	0.080	5,478	5,565	4,300	6,224	4,300	4,300	12	5	5	68,3
	AAEL007078	0.172	0.074	5,802	6,426	4,300	5,951	4,300	5,760	2	13	13	133,3
	AAEL001411	0.166	0.216	4,788	4,976	4,300	4,965	4,300	4,300	1	15	15	227,0
	AAEL005843	0.166	0.106	5,370	5,798	4,300	5,312	4,300	5,359	13	8	8	251,5
	AAEL019604	0.165	0.200	6,504	6,241	5,611	6,306	5,742	5,813	3	10	10	54,1
	AAEL004338	0.164	0.085	4,300	5,975	4,300	5,482	4,300	4,300	1	4	4	38,5
	AAEL021134	0.162	0.070	5,932	6,261	4,300	6,127	4,300	5,579	2	11	3	80,6
	AAEL028021	0.161	0.427	4,300	4,784	4,300	4,300	4,300	4,300	7	2	2	79,4
	AAEL010004	0.161	0.106	4,300	5,677	4,300	4,300	4,300	5,194	2	6	6	81,2
	AAEL024235	0.161	0.114	5,402	5,561	4,300	5,372	4,300	5,108	8	16	16	298,0
dab2-interacting protein	AAEL001009	0.159	0.427	4,300	4,778	4,300	4,300	4,300	4,300	1	3	3	94,2
	AAEL020485	0.158	0.427	4,300	4,774	4,300	4,300	4,300	4,300	1	2	2	20,7
	AAEL002542	0.157	0.076	5,547	5,371	4,300	6,146	4,300	4,300	1	4	4	26,3
	AAEL012243	0.157	0.092	5,733	5,667	4,300	5,427	4,300	5,503	1	7	7	83,4
	AAEL022136	0.155	0.103	5,278	5,767	4,300	5,269	4,300	5,309	8	3	3	57,3
	AAEL012661	0.145	0.082	5,545	5,902	4,300	5,477	4,300	5,534	1	3	3	30,4
	AAEL017437	0.144	0.077	4,300	5,889	4,300	4,300	4,300	5,456	2	6	6	57,4
	AAEL004500	0.141	0.046	6,485	6,557	4,300	6,800	4,300	5,820	4	12	12	94,4
	AAEL012943	0.139	0.094	5,505	5,542	4,300	5,354	4,300	5,275	1	3	3	48,6
	AAEL014715	0.138	0.076	5,850	5,636	4,300	5,497	4,300	5,573	1	10	10	63,5
	AAEL013071	0.136	0.069	5,869	5,830	4,300	5,785	4,300	5,507	1	3	3	52,2
	AAEL001061	0.130	0.046	5,639	5,874	4,300	6,822	4,300	4,300	3	5	3	23,8
	AAEL010821	0.129	0.222	7,434	7,483	7,765	7,374	7,116	7,806	1	13	13	33,8
	AAEL009646	0.129	0.050	5,845	6,602	4,300	6,108	4,300	5,953	2	8	8	66,3
	AAEL002906	0.129	0.078	5,305	5,148	4,300	5,767	4,300	4,300	1	5	5	111,3
	AAEL023255	0.125	0.059	5,747	5,431	4,300	6,181	4,300	4,622	2	9	9	95,7
	AAEL010403	0.125	0.081	5,514	5,579	4,300	5,345	4,300	5,374	2	6	6	61,4
	AAEL002334	0.125	0.068	5,236	6,068	4,300	5,397	4,300	5,533	1	6	6	51,0
	AAEL007699	0.124	0.046	6,470	6,212	4,300	6,096	4,300	6,215	3	5	5	21,4
	AAEL005515	0.124	0.050	4,300	6,285	4,300	5,913	4,300	4,300	4	7	7	29,8
	AAEL002748	0.124	0.091	5,511	5,310	4,300	5,212	4,300	5,238	3	4	4	59,8
	AAEL007778	0.116	0.053	5,850	6,095	4,300	5,928	4,300	5,670	1	7	7	64,6
	AAEL013069	0.114	0.043	6,103	6,511	4,300	6,050	4,300	6,221	1	10	10	34,9
	AAEL001913	0.112	0.074	5,636	5,343	4,300	5,268	4,300	5,376	2	5	5	37,8
	AAEL02359	0.099	0.031	5,628	6,073	4,300	7,104	4,300	4,300	2	5	5	18,5
	AAEL019986	0.098	0.065	4,300	5,543	4,300	5,250	4,300	4,300	12	3	3	156,4
	AAEL011116	0.098	0.037	5,823	5,409	4,300	6,639	4,300	4,300	1	5	4	29,5
	AAEL018120	0.098	0.058	5,695	5,509	4,300	5,413	4,300	5,498	7	5	5	62,0
	AAEL003427	0.097	0.034	6,422	6,439	4,300	6,095	4,300	6,474	1	10	10	16,7
	AAEL006942	0.094	0.048	5,590	5,916	4,300	5,501	4,300	5,723	4	6	6	67,8
	AAEL010991	0.092	0.071	4,300	5,383	4,300	5,108	4,300	4,300	4	5	5	79,2
	AAEL009287	0.089	0.106	6,229	6,422	7,094	6,516	6,216	6,747	2	6	6	24,5
	AAEL011180	0.081	0.039	5,396	6,126	4,300	5,827	4,300	5,453	1	4	4	31,0
	AAEL004855	0.080	0.030	6,149	6,437	4,300	6,125	4,300	6,220	2	8	8	33,0
	AAEL008517	0.079	0.031	6,061	6,347	4,300	5,337	4,300	4,300	2	3	3	258,8
	AAEL004472	0.079	0.026	6,389	6,607	4,300	6,255	4,300	6,504	3	17	15	86,9
	AAEL005528	0.079	0.051	5,438	5,519	4,300	5,247	4,300	5,473	4	3	3	79,9
	AAEL027978	0.077	0.092	4,983	4,511	4,300	4,962	4,300	4,300	44	2	2	219,2
	AAEL007565	0.077	0.053	4,920	5,186	4,300	5,574	4,300	4,300	1	5	5	155,4
	AAEL009182	0.076	0.060	6,833	7,258	5,977	6,755	6,167	6,917	1	16	16	26,9
	AAEL009894	0.076	0.079	4,300	5,121	4,300	4,893	4,300	4,300	2	2	2	42,9
	AAEL019783	0.073	0.058	5,222	6,434	4,300	5,337	4,300	4,300	2	3	3	258,8
	AAEL017315	0.067	0.033	5,349	5,226	4,300	6,075	4,300	4,300	2	4	4	90,3
	AAEL006050	0.066	0.038	4,300	5,943	4,300	4,969	4,300	5,075	1	4	4	107,2
	AAEL009151	0.063	0.021	6,374	6,542	4,300	6,416	4,300	6,312	1	4	4	14,8
	AAEL023850	0.061	0.027	6,045	5,865	4,300	5,809	4,300	5,917	1	9	9	183,5
	AAEL013344	0.058	0.025	6,064	5,861	4,300	5,994	4,300	5,757	2	2	2	21,9
	AAEL003872	0.056	0.029	4,300	5,787	4,300	5,618	4,300	4,300	1	3	3	19,6
	AAEL018323	0.055	0.023	6,121	6,009	4,300	6,038	4,300	5,927	1	8	1	93,0
	AAEL012875	0.050	0.024	4,300	5,860	4,300	5,710	4,300	4,300	1	6	6	24,5
	AAEL010754	0.049	0.033	4,300	5,429	4,300	5,282	4,300	4,300	3	3	3	12,5
	AAEL005817	0.049	0.022	5,785	5,969	4,300	5,646	4,300	5,962	1	8	8	17,4
	AAEL013536	0.049	0.031	5,444	5,493	4,300	5,316	4,300	5,476	3	5	3	18,0
	AAEL006634	0.047	0.026	5,778	5,366	4,300	5,705	4,300	5,299	1	3	3	43,3
	AAEL003393	0.042	0.016	5,803	6,420	4,300	6,161	4,300	5,937	2	9	9	54,0
	AAEL014843	0.040	0.013	6,464	6,461	4,300	6,958	4,300	5,847	2	15	15	81,5
	AAEL007707	0.039	0.024	5,058	5,116	4,300	5,757	4,300	4,300	2	3	3	35,7
	AAEL022104	0.037	0.013	6,236	6,486	4,300	6,446	4,300	6,164	1	8	8	46,8
	AAEL006095	0.031	0.012	6,043	5,729	4,300	6,519	4,300	5,160	4	10	10	83,6
	AAEL009987	0.030	0.012	6,012	6,243	4,300	6,007	4,300	6,156	1	7	7	28,6
	AAEL008073	0.030	0.009	6,325	6,772	4,300	6,735	4,300	6,270	1	12	12	47,6
	AAEL026804	0.030	0.017	5,235	5,003	4,300	5,849	4,300	4,300	1	6	6	146,2
	AAEL004297	0.029	0.011	5,982	5,714	4,300	6,564	4,300	5,045	10	11	11	119,2
	AAEL003582	0.027	0.009	6,204	6,595	4,300	6,243	4,300	6,476	1	7	7	17,2
	AAEL008687	0.026	0.027	6,839	7,052	7,614	7,025	6,819	7,583	3	12	12	41,6
	AAEL005669	0.024	0.011	5,880	5,585	4,300	6,114	4,300	5,281	1	2	2	22,8
	AAFL012010	0.021	0.012	5,618	5,594	4,300	5,535	4,300	5,613	1	2	2	16,4
	P00760 TRY	0.021	0.029	7,988	8,114	8,322	7,709	8,495	8,156	2	9	9	25,8
	AAEL019408	0.021	0.007	6,031	6,161	4,300	6,772	4,300	5,356	1	6	5	21,9
	AAEL009691	0.020	0.005	6,791	7,086	4,300	6,283	4,300	7,534	4	43	43	130,6
	AAEL002178												

AAEL010826	-0.040	0.023	4,300	5,493	4,300	5,613	4,300	4,300	2	6	6	51,3
AAEL009994	-0.041	0.013	6,189	6,736	4,300	6,479	4,300	6,567	1	15	15	48,9
AAEL014931	-0.041	0.038	4,300	5,003	4,300	4,300	4,300	5,126	8	5	5	122,3
AAEL015065	-0.041	0.014	6,349	6,281	4,300	6,396	4,300	6,357	4	59	59	278,0
AAEL023176	-0.042	0.019	5,565	6,002	4,300	6,116	4,300	5,578	2	4	4	30,7
AAEL002761	-0.045	0.034	4,300	5,175	4,300	5,311	4,300	4,300	39	3	3	29,1
AAEL022819	-0.047	0.020	5,586	6,175	4,300	6,256	4,300	5,646	2	8	8	191,5
AAEL019717	-0.049	0.032	5,424	5,244	4,300	5,590	4,300	5,225	2	2	2	38,3
AAEL006885	-0.051	0.028	6,988	6,570	5,641	7,358	6,036	5,958	7	9	8	28,2
AAEL002083	-0.053	0.036	4,300	5,582	4,300	4,869	4,300	5,174	1	8	4	75,4
AAEL002851	-0.063	0.064	5,936	6,442	5,746	5,985	5,703	6,626	2	14	3	50,1
AAEL014562	-0.063	0.130	7,166	6,873	7,091	6,853	7,074	7,392	1	4	4	17,6
AAEL013904	-0.064	0.031	4,300	5,655	4,300	5,847	4,300	4,300	1	4	4	33,9
AAEL020238	-0.064	0.023	4,300	6,163	4,300	6,354	4,300	4,300	1	5	5	31,4
AAEL006928	-0.065	0.054	4,300	5,088	4,300	5,284	4,300	4,300	1	2	2	53,7
AAEL013320	-0.069	0.044	5,408	5,322	4,300	5,544	4,300	5,392	1	3	3	18,2
AAEL004317	-0.073	0.127	6,447	6,236	6,815	6,336	6,624	6,755	1	9	9	64,0
AAEL022286	-0.073	0.028	5,705	6,368	4,300	6,276	4,300	6,016	1	2	2	9,4
AAEL008481	-0.075	0.026	6,243	6,269	4,300	6,394	4,300	6,342	2	7	7	22,0
AAEL005997	-0.075	0.030	5,337	5,351	4,300	6,615	4,300	4,300	2	7	7	14,8
AAEL013359	-0.080	0.030	5,968	6,168	4,300	6,502	4,300	5,874	1	8	8	45,6
AAEL005544	-0.085	0.060	5,279	5,275	4,300	5,380	4,300	5,421	5	3	3	93,3
AAEL012069	-0.086	0.038	5,632	5,374	4,300	6,428	4,300	4,834	3	6	6	19,0
AAEL005845	-0.088	0.031	6,397	6,108	4,300	6,360	4,300	6,409	1	57	57	276,4
AAEL000454	-0.089	0.051	5,334	5,619	4,300	5,669	4,300	5,550	2	3	3	38,8
AAEL022661	-0.090	0.045	5,599	5,752	4,300	5,929	4,300	5,692	6	20	20	88,1
AAEL002886	-0.100	0.057	5,099	4,880	4,300	5,979	4,300	4,300	4	3	3	54,0
AAEL022213	-0.102	0.115	4,300	4,811	4,300	5,116	4,300	4,300	2	3	3	45,4
AAEL001759	-0.116	0.036	6,229	6,740	4,300	6,640	4,300	6,677	1	9	9	22,8
AAEL010159	-0.120	0.063	4,300	5,510	4,300	5,871	4,300	4,300	1	7	7	124,1
AAEL017096	-0.123	0.030	7,051	7,228	4,300	7,680	4,300	6,967	5	12	12	50,5
AAEL012155	-0.125	0.095	4,300	5,472	4,300	5,106	4,300	5,041	1	3	3	68,9
K1C10_HUMA	-0.126	0.124	7,971	7,698	8,189	7,401	8,337	8,498	3	31	27	58,8
AAEL006048	-0.126	0.054	4,300	6,333	4,300	5,741	4,300	5,271	1	6	6	44,3
AAEL003130	-0.127	0.073	5,401	5,574	4,300	5,657	4,300	5,697	4	3	3	26,6
AAEL008341	-0.128	0.066	4,300	5,533	4,300	5,917	4,300	4,300	1	3	3	47,6
AAEL011471	-0.129	0.054	5,930	5,966	4,300	6,215	4,300	6,067	3	8	8	21,6
AAEL004325	-0.136	0.177	6,262	6,790	6,308	6,697	6,136	6,935	1	9	9	34,0
AAEL009606	-0.138	0.122	5,113	4,994	4,300	5,148	4,300	5,373	3	3	3	76,6
AAEL010585	-0.138	0.049	6,077	6,325	4,300	6,645	4,300	6,172	1	19	19	88,8
AAEL000424	-0.139	0.119	4,772	4,614	4,300	5,502	4,300	4,300	1	2	2	54,9
AAEL007288	-0.141	0.119	4,300	5,355	4,300	4,932	4,300	5,148	3	5	5	94,3
AAEL006946	-0.144	0.091	5,307	5,280	4,300	5,874	4,300	5,145	1	5	5	58,6
AAEL012686	-0.147	0.065	5,481	6,105	4,300	5,818	4,300	6,210	1	4	4	16,1
AAEL019789	-0.150	0.042	6,656	6,830	4,300	6,943	4,300	6,994	2	12	12	30,1
AAEL017030	-0.153	0.074	4,300	6,163	4,300	5,442	4,300	5,482	1	3	3	20,3
AAEL013346	-0.154	0.048	6,480	6,493	4,300	6,911	4,300	6,524	2	5	3	21,8
AAEL024434	-0.158	0.084	4,300	5,976	4,300	5,392	4,300	5,358	2	6	6	27,1
AAEL017516	-0.175	0.071	5,658	6,246	4,300	6,133	4,300	6,296	1	3	3	40,0
AAEL018211	-0.226	0.308	4,300	4,903	4,300	5,052	4,300	4,828	1	3	3	195,1
AAEL004563	-0.226	0.150	4,300	5,621	4,300	5,460	4,300	5,138	1	5	5	44,4
AAFL014583	-0.226	0.539	6,415	6,304	6,409	6,239	6,776	6,791	2	3	3	11,3
K2C1_HUMAN	-0.237	0.261	8,080	7,790	8,558	7,818	8,579	8,743	1	44	38	66,0
AAEL013407	-0.242	0.115	4,300	5,514	4,300	6,239	4,300	4,300	5	8	4	56,9
AAEL010340	-0.243	0.297	4,993	4,300	4,300	4,964	4,300	5,057	3	2	2	20,4
AAEL004902	-0.243	0.116	4,300	6,170	4,300	5,616	4,300	5,582	1	4	4	23,7
AAEL012545	-0.248	0.120	5,309	5,385	4,300	6,534	4,300	4,904	1	5	5	29,0
AAEL000641	-0.249	0.115	4,300	5,554	4,300	6,300	4,300	4,300	1	9	9	56,0
AAEL006833	-0.255	0.191	4,300	4,933	4,300	5,698	4,300	4,300	2	4	4	34,5
AAEL013279	-0.257	0.141	4,300	5,296	4,300	6,066	4,300	4,300	1	5	5	21,4
AAEL006511	-0.258	0.189	4,300	5,512	4,300	5,937	4,300	5,570	2	12	12	190,6
K22E_HUMAN	-0.224	0.170	7,773	6,998	7,886	6,952	8,139	8,239	2	35	27	65,4
K2CS_HUMAN	-0.225	0.226	6,971	6,470	7,397	6,653	7,242	7,617	2	31	20	62,4
AAEL018211	-0.226	0.308	4,300	4,903	4,300	5,052	4,300	4,828	1	3	3	195,1
AAEL004563	-0.226	0.150	4,300	5,621	4,300	5,460	4,300	5,138	1	5	5	44,4
AAEL014583	-0.226	0.539	6,415	6,304	6,409	6,239	6,776	6,791	2	3	3	11,3
K2C1_HUMAN	-0.237	0.261	8,080	7,790	8,558	7,818	8,579	8,743	1	44	38	66,0
AAEL013407	-0.242	0.115	4,300	5,514	4,300	6,239	4,300	4,300	5	8	4	56,9
AAEL010340	-0.243	0.297	4,993	4,300	4,300	4,964	4,300	5,057	3	2	2	20,4
AAEL004902	-0.243	0.116	4,300	6,170	4,300	5,616	4,300	5,582	1	4	4	23,7
AAEL012545	-0.248	0.120	5,309	5,385	4,300	6,534	4,300	4,904	1	5	5	29,0
AAEL000641	-0.249	0.115	4,300	5,554	4,300	6,300	4,300	4,300	1	9	9	56,0
AAEL006833	-0.255	0.191	4,300	4,933	4,300	5,698	4,300	4,300	2	4	4	34,5
AAEL013279	-0.257	0.141	4,300	5,296	4,300	6,066	4,300	4,300	1	5	5	21,4
AAEL006511	-0.258	0.189	4,300	5,512	4,300	5,937	4,300	5,570	2	12	12	190,6
AAEL001005	-0.263	0.113	5,129	5,074	4,300	6,691	4,300	4,300	1	4	4	46,7
AAEL008878	-0.282	0.246	4,300	5,299	4,300	5,219	4,300	5,225	1	3	3	68,2
AAEL003957	-0.303	0.110	6,169	5,901	4,300	7,089	5,890	4,300	2	7	7	17,1
AAEL010146	-0.303	0.223	4,300	5,492	4,300	5,406	4,300	5,296	1	5	5	82,5
AAEL01C14_HUMA	-0.305	0.223	6,897	5,621	7,227	6,471	7,165	7,023	1	24	10	51,6
AAEL015100	-0.312	0.297	4,300	5,152	4,300	5,384	4,300	5,004	5	3	3	68,5
AAEL008152	-0.313	0.244	4,621	4,532	4,300	5,791	4,300	4,300	3	3	3	27,1
PLAK_HUMAN	-0.328	0.448	5,467	5,388	6,043	5,489	6,143	6,250	10	11	11	81,7
K1C9_HUMAN	-0.330	0.292	7,837	6,959	8,224	7,480	8,275	8,254	1	22	21	62,1
AAEL005266	-0.332	0.149	6,441	6,867	4,300	6,361	5,717	6,526	2	10	10	16,3
AAEL000758	-0.332	0.176	5,143	4,997	4,300	6,459	4,300	4,678	1	10	10	12,1
AAEL008848	-0.333	0.227	4,300	5,579	4,300	5,519	4,300	5,359	1	4	4	32,8
K1C16_HUMA	-0											

Table S3. Mass Spec data WNV

Name (some based on orthology with <i>Drosophila</i>)	Log LFQ (protein abundance)												
	Gene IDs	Log difference	-Log=(P-value)	WNV-sfRNA 1	WNV-sfRNA 2	WNV-sfRNA 3	NS2A 1	NS2A 2	NS2A 3	Proteins (#)	Peptides (#)	Unique peptides (#)	Mw (kDa)
Me31b	AAEL008500	2,407	2,852	7,340	6,972	7,436	5,098	4,300	5,128	2	28	28	50,4
Ataxin-2	AAEL007805	1,602	1,806	5,698	6,526	6,391	5,208	4,300	4,300	6	11	11	104,2
Rp519	AAEL010756	1,590	1,049	6,664	6,475	6,660	6,428	4,300	4,300	3	9	9	17,3
Protein lingerer	AAEL009607	1,390	0,927	4,300	6,537	6,234	4,300	4,300	4,300	16	4	4	127,4
RpL23	AAEL015006	1,378	0,887	5,981	4,300	6,752	4,300	4,300	4,300	1	5	5	14,9
RpS10	AAEL002047	1,253	0,922	6,356	4,300	6,003	4,300	4,300	4,300	1	4	4	18,0
SAV_STRAV	AAEL012399	1,239	0,587	8,909	7,807	9,166	8,200	5,700	8,265	1	4	4	18,8
RpL38	AAEL005451	1,184	0,935	6,104	4,300	6,048	4,300	4,300	4,300	1	3	3	8,3
	AAEL008103	1,127	0,743	6,945	6,036	7,014	6,233	4,300	6,080	1	11	11	23,4
Tubulin	AAEL002848	1,092	0,686	6,944	6,367	6,978	6,148	4,300	6,566	1	14	5	50,8
RpL1P1	AAEL005027	1,082	0,924	6,065	4,300	5,782	4,300	4,300	4,300	5	4	4	11,5
RpL10a	AAEL013221	1,045	0,490	7,285	6,916	7,284	6,771	4,300	7,279	2	8	8	24,6
Lsm12	AAEL007820	1,037	0,916	5,680	4,300	6,032	4,300	4,300	4,300	1	2	2	20,6
AAEL018126	AAEL018126	1,026	3,406	5,223	5,513	5,242	4,300	4,300	4,300	14	6	6	177,1
	AAEL005515	1,026	0,858	6,121	5,831	5,639	5,913	4,300	4,300	4	7	7	29,8
ATP synthase alpha	AAEL012175	1,025	0,612	6,869	6,071	7,120	6,275	4,300	6,409	1	13	13	59,4
Prohibitin	AAEL009691	1,011	0,432	7,671	6,500	6,980	6,283	4,300	7,534	4	43	43	130,6
RNA and export factor binding protein 2	AAEL026243	1,002	0,683	6,452	6,204	6,924	5,857	4,300	6,415	4	8	8	39,0
	AAEL019669	0,953	1,040	5,547	5,847	5,627	4,300	4,300	5,563	1	5	5	39,6
	AAEL013069	0,928	0,639	6,415	6,073	6,868	6,050	4,300	6,221	1	10	10	34,9
	AAEL025999	0,926	0,647	6,151	4,300	5,997	4,300	4,300	5,070	2	2	2	15,2
	AAEL011447	0,923	0,734	6,432	6,155	6,458	5,855	4,300	6,121	1	8	8	20,5
arginyl-tRNA synthetase	AAEL000199	0,920	0,930	5,603	4,300	5,758	4,300	4,300	4,300	1	7	7	75,6
	AAEL008738	0,904	0,769	6,417	6,157	6,213	5,743	4,300	6,032	1	13	10	98,9
Heat shock cognate 70	AAEL002823	0,885	0,405	6,470	4,300	6,502	4,300	4,300	4,300	1	3	3	27,3
	AAEL019403	0,877	0,484	6,823	6,589	6,721	6,893	4,300	6,309	3	18	14	71,1
	AAEL003396	0,863	0,643	6,389	5,848	6,617	6,008	4,300	5,957	1	6	6	15,8
	AAEL015065	0,859	0,465	7,310	6,354	5,966	6,396	4,300	6,357	4	59	59	278,0
	AAEL021422	0,852	0,821	5,192	4,300	5,963	4,300	4,300	4,300	2	3	3	21,2
	AAEL020447	0,843	0,530	6,634	6,141	6,635	6,563	4,300	6,017	3	5	5	13,4
Otefin	AAEL001580	0,840	0,927	5,466	4,300	5,654	4,300	4,300	4,300	1	4	4	45,6
	AAEL007771	0,839	0,459	6,881	6,287	6,840	6,642	4,300	6,549	1	6	6	17,6
cdk1	AAEL008621	0,819	0,931	5,466	4,300	5,591	4,300	4,300	4,300	3	2	2	34,6
	AAEL008658	0,817	0,681	6,361	5,418	6,282	5,738	4,300	5,572	1	9	9	79,6
	AAEL009994	0,801	0,434	6,765	6,043	6,942	6,479	4,300	6,567	1	15	15	48,9
CTP synthase	AAEL005455	0,801	0,935	5,487	4,300	5,516	4,300	4,300	4,300	2	2	2	73,5
	AAEL010296	0,790	0,544	6,159	5,908	6,164	5,088	4,300	6,474	1	9	9	77,2
	AAEL022104	0,781	0,498	6,446	6,188	6,619	6,446	4,300	6,164	1	8	8	46,8
	AAEL002372	0,779	0,475	6,378	5,504	6,823	5,778	4,300	6,289	1	5	5	17,6
	AAEL011180	0,778	0,713	6,320	5,650	5,944	5,827	4,300	5,453	1	4	4	31,0
	AAEL021386	0,778	0,885	5,246	4,300	5,689	4,300	4,300	4,300	2	2	2	23,8
	AAEL005845	0,777	0,409	7,237	6,331	5,834	6,360	4,300	6,409	1	57	57	276,4
	AAEL011870	0,774	0,881	5,818	6,052	5,720	5,408	4,300	5,560	3	8	8	55,9
elF3k	AAEL006115	0,770	0,933	5,500	4,300	5,409	4,300	4,300	4,300	1	2	2	25,8
RpL10	AAEL025362	0,766	0,376	6,802	6,285	7,048	6,729	4,300	6,808	2	6	6	25,4
	AAEL023176	0,755	0,605	5,910	5,962	6,388	6,116	4,300	5,578	2	4	4	30,7
	AAEL007699	0,751	0,517	6,409	5,984	6,471	6,096	4,300	6,215	3	5	5	21,4
	AAEL003582	0,750	0,442	6,606	5,959	6,703	6,243	4,300	6,476	1	7	7	17,2
	AAEL021134	0,747	0,506	6,789	5,729	5,731	6,127	4,300	5,579	2	11	3	80,6
	AAEL0013982	0,747	0,794	5,998	5,603	5,966	5,347	4,300	5,679	1	6	6	38,0
	AAEL017096	0,729	0,286	7,016	7,017	7,102	7,680	4,300	6,967	5	12	12	50,5
	AAEL004699	0,728	0,521	6,182	6,110	6,313	6,355	4,300	5,764	3	16	16	112,0
	AAEL015187	0,728	0,476	6,349	5,852	6,611	6,053	4,300	6,275	1	2	2	16,0
Vap33	AAEL024800	0,720	0,935	5,397	4,300	5,365	4,300	4,300	4,300	2	2	2	31,1
	AAEL008517	0,719	0,515	6,219	5,958	6,448	6,089	4,300	6,080	1	9	9	51,1
	AAEL009646	0,718	0,542	6,322	6,022	6,169	6,108	4,300	5,953	2	8	8	66,3
fuse-binding protein-interacting repressor	AAEL004415	0,716	0,812	5,035	4,300	5,712	4,300	4,300	4,300	5	5	5	64,1
	AAEL017516	0,712	0,456	6,325	5,908	6,632	6,133	4,300	6,296	1	3	3	40,0
	AAEL001769	0,708	0,586	6,228	5,546	6,199	5,761	4,300	5,787	1	13	11	78,8
	AAEL002525	0,698	0,859	5,584	5,902	5,667	5,489	4,300	5,272	4	15	15	214,4
	AAEL003993	0,695	0,480	5,909	4,300	5,824	5,348	4,300	4,300	1	6	6	31,5
La related protein	AAEL009070	0,692	0,886	5,299	5,332	5,430	5,385	4,300	4,300	3	5	5	169,5
	AAEL008329	0,689	0,548	5,932	5,440	6,257	5,225	4,300	6,039	1	3	3	17,4
	AAEL006091	0,682	0,931	5,270	4,300	5,376	4,300	4,300	4,300	3	2	2	23,5
rab6	AAEL024040	0,676	0,536	5,740	4,300	5,734	4,300	4,300	4,300	2	2	2	27,0
elF3i	AAEL013144	0,675	0,932	5,357	4,300	5,269	4,300	4,300	4,300	1	4	4	36,0
	AAEL008073	0,667	0,373	6,564	6,323	6,420	6,735	4,300	6,270	1	12	12	47,6
	AAEL010754	0,665	0,486	5,729	4,300	5,848	5,282	4,300	4,300	3	3	3	12,5
	AAEL007778	0,660	0,582	5,926	6,025	5,928	5,928	4,300	5,670	1	7	7	64,6
	AAEL023188	0,660	0,917	5,180	4,300	5,401	4,300	4,300	4,300	1	3	3	68,1
	AAEL000217	0,643	0,848	5,015	4,300	5,515	4,300	4,300	4,300	3	4	4	109,7
serine/threonine protein kinase	AAEL000318	0,638	1,645	7,032	7,310	6,758	6,474	6,241	6,470	2	27	27	69,7
	AAEL005817	0,634	0,529	5,892	5,725	6,191	5,646	4,300	5,962	1	8	8	17,4
	AAEL025547	0,633	0,920	5,152	4,300	5,347	4,300	4,300	4,300	1	3	3	93,3
Cytochrome B5	AAEL0010017	0,633	0,909	5,122	4,300	5,376	4,300	4,300	4,300	1	2	2	14,7
	AAEL012827	0,632	0,535	5,975	5,804	5,932	6,071	4,300	5,443	1	10	10	91,1
	AAEL006958	0,626	0,778	4,894	4,300	5,584	4,300	4,300	4,300	3	2	2	145,2
Rp135	AAEL000823	0,624	0,302	6,234	4,300	5,980	6,042	4,300	4,300	1	4	4	16,9
	AAEL000982	0,623	0,468	6,114	5,513	6,274	5,726	4,300	6,004	1	5	5	39,4
	AAEL009897	0,620	0,434	5,994	5,939	6,392	6,007	4,300	6,156	1</td			

	AAEL012359	0.500	0.190	5,943	6,242	5,018	7,104	4,300	4,300	2	5	5	18.5
	AAEL010159	0.498	0.403	5,332	5,366	5,267	5,871	4,300	4,300	1	7	7	124,1
	AAEL021083	0.497	0.254	6,262	4,300	6,284	5,635	4,300	5,421	1	3	3	13,4
	AAEL019789	0.492	0.213	6,718	6,372	6,622	6,943	4,300	6,994	2	12	12	30,1
Chaperonin	AAEL000486	0.491	0.340	5,468	5,551	5,097	6,043	4,300	4,300	1	6	6	59,6
	AAEL006315	0.490	0.315	5,631	4,300	5,746	5,607	4,300	4,300	3	7	7	99,3
	AAEL010778	0.489	0.524	5,365	4,300	5,341	4,939	4,300	4,300	5	2	2	34,6
	AAEL013344	0.482	0.373	5,621	6,001	5,875	5,994	4,300	5,757	2	2	2	21,9
	AAEL006048	0.480	0.488	5,698	5,520	5,534	5,741	4,300	5,271	1	6	6	44,3
	AAEL024434	0.476	0.271	5,919	4,300	6,259	5,392	4,300	5,358	2	6	6	27,1
	AAEL012586	0.475	0.929	5,060	4,300	4,966	4,300	4,300	4,300	1	3	3	15,6
Eukaryotic translation initiation factor 3 subunit H	AAEL007945	0.466	0.622	5,569	5,378	5,284	5,178	4,300	5,356	1	4	3	38,5
	AAEL010467	0.459	0.675	5,443	5,356	5,313	5,177	4,300	5,257	1	5	5	39,8
	AAEL025697	0.455	0.334	5,635	6,132	5,522	6,102	4,300	5,521	1	9	8	72,7
	AAEL003726	0.451	0.918	4,903	4,300	5,051	4,300	4,300	4,300	1	2	2	61,8
	AAEL008192	0.446	0.762	7,001	6,845	7,331	6,755	6,167	6,917	1	16	16	26,9
	AAEL020749	0.445	0.196	6,310	4,300	6,564	5,635	4,300	5,904	1	6	6	17,1
	AAEL017437	0.444	0.322	5,528	4,300	5,561	4,300	4,300	5,456	2	6	6	57,4
	AAEL012875	0.443	0.271	5,723	4,300	5,616	5,710	4,300	4,300	1	6	6	24,5
	AAEL012122	0.443	0.423	5,240	4,300	5,480	5,093	4,300	4,300	1	6	6	56,3
	AAEL002851	0.442	0.655	5,675	6,295	6,770	5,985	5,703	6,626	2	14	3	50,1
	AAEL001411	0.438	0.264	6,204	4,300	4,375	4,965	4,300	4,300	1	15	15	227,0
	AAEL010004	0.437	0.363	5,111	4,300	5,695	4,300	4,300	5,194	2	6	6	81,2
	AAEL018323	0.436	0.308	5,604	5,908	6,062	6,038	4,300	5,927	1	8	1	93,0
Nup358	AAEL020592	0.434	0.306	5,395	4,300	5,689	5,482	4,300	4,300	4	7	7	292,2
calponin/transgelin	AAEL004500	0.429	0.225	6,260	6,208	5,739	6,800	4,300	5,820	4	12	12	94,4
	AAEL006922	0.428	0.284	5,334	5,701	4,786	5,938	4,300	4,300	1	3	3	20,7
	AAEL006977	0.421	0.351	5,673	5,479	5,749	5,985	4,300	5,353	1	6	6	66,3
	AAEL012661	0.411	0.436	5,464	5,599	5,481	5,477	4,300	5,534	1	3	3	30,4
	AAEL006794	0.404	0.181	6,266	4,300	6,453	5,937	4,300	5,570	2	12	12	190,6
	AAEL009475	0.404	0.373	5,307	4,300	5,377	4,300	4,300	5,173	1	6	6	246,7
	AAEL004338	0.399	0.288	5,474	4,300	5,504	5,482	4,300	4,300	1	4	4	38,5
	AAEL011656	0.397	0.183	6,460	6,024	6,454	6,872	4,300	6,576	1	5	5	17,0
	AAEL024235	0.396	0.236	6,290	4,300	5,379	5,372	4,300	5,108	8	16	16	298,0
	AAEL022213	0.393	0.378	5,435	5,161	5,161	5,116	4,300	4,300	2	3	3	45,4
	AAEL009894	0.393	0.475	5,102	4,300	5,268	4,893	4,300	4,300	2	2	2	42,9
	AAEL005097	0.391	0.168	6,309	4,300	6,535	5,773	4,300	5,898	1	5	5	25,1
	AAEL017481	0.391	0.270	5,743	6,094	5,387	6,113	4,300	5,638	1	6	6	18,7
	AAEL013346	0.390	0.181	6,113	6,456	6,336	6,911	4,300	6,524	2	5	3	21,8
	AAEL010248	0.381	0.285	5,718	4,300	5,658	5,039	4,300	5,193	1	3	3	33,7
	AAEL012243	0.380	0.411	5,395	5,567	5,407	5,427	4,300	5,503	1	7	7	83,4
	AAEL009185	0.379	0.197	5,625	6,162	5,516	6,732	4,300	5,133	7	10	10	39,9
translational activator gcn1	AAEL006187	0.379	0.935	4,862	4,300	4,876	4,300	4,300	4,300	1	3	3	293,3
	AAEL013359	0.366	0.213	5,745	5,856	6,173	6,502	4,300	5,874	1	8	8	45,6
	AAEL000270	0.359	0.311	5,381	4,300	5,266	5,271	4,300	4,300	1	3	3	37,9
	AAEL004546	0.359	0.923	4,789	4,300	4,887	4,300	4,300	4,300	1	2	2	107,1
	AAEL019604	0.357	0.811	6,292	6,492	6,147	6,306	5,742	5,813	3	10	10	54,1
	AAEL013625	0.347	0.161	6,334	5,958	6,431	6,639	4,300	6,743	1	9	9	24,6
	AAEL014931	0.347	0.332	5,430	4,300	5,035	4,300	4,300	5,126	8	5	5	122,3
	AAEL012585	0.345	0.118	6,699	4,300	6,906	6,244	4,300	6,325	1	7	7	30,3
	AAEL013904	0.334	0.187	5,797	4,300	5,351	5,847	4,300	4,300	1	4	4	33,9
	AAEL002761	0.327	0.276	5,207	5,384	4,300	5,311	4,300	4,300	39	3	3	29,1
	AAEL019555	0.326	0.170	5,305	5,922	4,300	5,950	4,300	4,300	2	7	7	142,8
	AAEL019549	0.325	0.186	5,395	4,300	5,717	5,836	4,300	4,300	6	6	6	141,5
	AAEL023850	0.324	0.239	5,495	5,623	5,881	5,809	4,300	5,917	1	9	9	183,5
	AAEL004855	0.322	0.117	6,545	4,300	6,676	6,125	4,300	6,220	2	8	8	33,0
	AAEL009496	0.315	0.115	6,506	4,300	6,741	6,206	4,300	6,096	1	6	6	22,1
	AAEL019986	0.314	0.277	5,399	4,300	5,093	5,250	4,300	4,300	12	3	3	156,4
ebna2 binding protein P100	AAEL000293	0.308	0.227	5,307	5,404	4,300	5,487	4,300	4,300	1	4	4	103,4
	AAEL007288	0.307	0.258	5,523	4,300	5,479	4,932	4,300	5,148	3	5	5	94,3
chaperonin-60kD	AAEL011584	0.307	0.168	5,489	6,161	4,835	6,258	4,300	5,008	1	11	11	60,8
	AAEL025553	0.306	0.248	5,206	5,383	4,300	5,370	4,300	4,300	1	5	5	71,6
cathepsin l	AAEL002833	0.305	0.167	5,569	5,568	4,300	5,923	4,300	4,300	1	4	4	38,0
	AAEL015100	0.304	0.358	5,113	5,503	4,984	5,384	4,300	5,004	5	3	3	68,5
proliferation-associated 2g4	AAEL012312	0.304	0.158	5,553	5,678	4,300	6,020	4,300	4,300	1	8	8	48,0
	AAEL001061	0.301	0.107	6,075	5,950	4,300	6,822	4,300	4,300	3	5	3	23,8
	AAEL000175	0.299	0.232	5,391	5,358	5,829	5,468	4,300	5,915	1	9	9	106,1
	AAEL022286	0.286	0.105	6,532	4,300	6,617	6,276	4,300	6,016	1	2	2	9,4
	AAEL003046	0.286	0.177	5,791	5,885	5,409	6,330	4,300	5,598	1	9	9	115,1
	TRY1_BOVIN	0.275	0.503	8,282	8,371	8,533	7,709	8,495	8,156	2	9	9	25,8
	AAEL024947	0.265	0.932	4,679	4,300	4,716	4,300	4,300	4,300	2	2	2	41,1
	AAEL009169	0.259	0.933	4,703	4,300	4,673	4,300	4,300	4,300	12	2	2	93,1
	K1C10_HUMA	0.254	0.286	8,551	8,256	8,191	7,401	8,337	8,498	3	31	27	58,8
	AAEL014526	0.252	0.301	5,107	5,193	5,339	5,212	4,300	5,369	1	3	3	35,7
	AAEL010826	0.252	0.170	5,282	4,300	5,385	5,613	4,300	4,300	2	6	6	51,3
	AAEL024500	0.251	0.924	4,644	4,300	4,709	5,423	4,300	5,498	7	5	5	62,0
	AAEL006928	0.250	0.202	4,834	5,499	4,300	5,284	4,300	4,300	1	2	2	53,7
	AAEL009747	0.229	0.270	7,114	6,617	7,116	7,146	6,150	6,864	1	10	10	17,5
	AAEL008848	0.223	0.130	5,614	4,300	5,932	5,519	4,300	5,359	1	4	4	32,8
	AAEL020485	0.219	0.808	4,523	4,300	4,734	4,300	4,300	4,300	1	2	2	20,7
	AAEL028021	0.217	0.932	4,642	4,300	4,610	4,300	4,300	4,300	7	2	2	79,4
	AAEL004563	0.216	0.143	5,628	4,300	5,618	5,460	4,300	5,138	1	5	5	44,4
	AAEL023265	0.216	0.119	5,665	4,300	6,157	5,376	4,300	5,374	2	10	10	146,6
	AAEL006474	0.205	0.746	4,481	4,300	4,735	4,300	4,300	4,3				

	AAEL001759	0.117	0.034	6,716	4,300	6,953	6,640	4,300	6,677	1	9	9	22,8
	AAEL007565	0.114	0.080	5,142	4,300	5,074	5,574	4,300	4,300	1	5	5	155,4
	AAEL004297	0.112	0.055	5,118	5,853	5,274	6,564	4,300	5,045	10	11	11	119,2
	AAEL013536	0.107	0.067	5,538	4,300	5,575	5,316	4,300	5,476	3	5	3	18,0
	AAEL005766	0.103	0.045	5,363	5,597	4,300	6,351	4,300	4,300	2	7	7	39,1
	AAEL001061	0,100	0.037	5,500	5,770	4,300	6,669	4,300	4,300	1	6	4	23,8
	AAEL007845	0.097	0.054	5,423	4,300	5,839	5,653	4,300	5,320	11	3	3	23,6
	AAEL012746	0.095	0.055	5,402	4,300	4,973	5,790	4,300	4,300	1	9	9	59,5
	AAEL008787	0.079	0.058	5,264	4,300	5,416	5,219	4,300	5,225	1	3	3	68,2
K22E_HUMAN	0,078	0.061	7,647	8,150	7,765	6,952	8,139	8,239	2	35	27	65,4	
AAEL023552	0,077	0.042	5,688	4,300	5,545	5,193	4,300	5,807	4	3	3	35,7	
AAEL009422	0.075	0.039	5,685	4,300	5,764	5,505	4,300	5,723	4	6	6	67,8	
AAEL002639	0.075	0.032	5,958	4,300	6,090	6,099	4,300	5,724	2	4	4	13,3	
K2C1_HUMAN	0,075	0.085	8,516	8,213	8,634	7,818	8,579	8,743	1	44	38	66,0	
AAEL002748	0.070	0.052	5,244	4,300	5,416	5,212	4,300	5,238	3	4	4	59,8	
AAEL01314	0.069	0.042	5,489	4,300	5,492	5,617	4,300	5,158	1	2	2	51,9	
AAEL010821	0,063	0.100	7,503	7,672	7,310	7,374	7,116	7,806	1	13	13	33,8	
AAEL013407	0,060	0.027	5,173	5,546	4,300	6,239	4,300	4,300	5	8	4	56,9	
AAEL023983	0.059	0.077	6,251	6,242	6,523	6,443	5,787	6,610	1	10	10	29,6	
AAEL007038	0.058	0.031	5,414	4,300	5,869	5,488	4,300	5,621	1	5	5	63,1	
AAEL011527	0.058	0.057	4,434	4,300	4,339	4,300	4,300	4,300	2	2	2	36,2	
AAEL001913	0.057	0.038	5,510	4,300	5,305	5,268	4,300	5,376	2	5	5	37,8	
AAEL014715	0.056	0.031	5,685	4,300	5,553	5,497	4,300	5,573	1	10	10	63,5	
AAEL006751	0.056	0.035	5,368	4,300	5,516	5,142	4,300	5,576	1	6	6	71,9	
AAEL007650	0.051	0.034	5,455	4,300	5,301	4,300	4,300	1	4	4	57,9		
AAEL026804	0.047	0.026	4,906	5,385	4,300	5,849	4,300	4,300	1	6	6	146,2	
AAEL003750	0,047	0.019	5,663	5,200	4,300	6,422	4,300	4,300	1	4	4	19,4	
AAEL012069	0.046	0.023	5,203	5,633	4,863	6,428	4,300	4,834	3	6	6	19,0	
AAEL009041	0.043	0.764	4,390	4,300	4,340	4,300	4,300	4,300	3	2	2	19,7	
AAEL005722	0.038	0.052	6,632	6,192	6,711	6,668	6,092	6,662	1	13	13	30,7	
AAEL002906	0,035	0.021	5,244	4,300	4,927	5,767	4,300	4,300	1	5	5	111,3	
AAEL005843	0,035	0.023	5,435	4,300	5,339	5,312	4,300	5,359	13	8	8	251,5	
AAEL017315	0,033	0.016	5,082	5,392	4,300	6,075	4,300	4,300	2	4	4	90,3	
AAEL009287	0,032	0.054	6,303	6,770	6,502	6,516	6,216	6,747	2	6	6	24,5	
AAEL011194	0,032	0.013	5,373	5,458	4,300	6,434	4,300	4,300	1	9	9	265,0	
AAEL013320	0,027	0.016	5,451	4,300	5,566	5,544	4,300	5,392	1	3	3	18,2	
AAEL007715	0,025	0.009	6,123	4,300	6,303	6,112	4,300	6,239	2	5	5	18,5	
AAEL011197	0,024	0.017	7,711	7,514	6,663	7,955	6,916	6,946	2	16	1	41,8	
AAEL008188	0,021	0.009	5,864	4,300	6,209	5,973	4,300	6,036	1	8	8	30,2	
AAEL006511	0,002	0.001	5,249	4,300	5,344	5,309	4,300	5,279	5	3	1	14,7	
protein disulfide-isomerase A6 precursor	AAEL010665	0,000	0.000	5,706	4,300	4,300	5,706	4,300	4,300	3	7	7	47,7
	AAEL027560	0,000	0.000	4,300	4,300	4,300	4,300	4,300	4,300	1	2	2	41,7
	AAEL010146	0,000	0.000	5,292	4,300	5,409	5,406	4,300	5,296	1	5	5	82,5
	CK2C5_HUMA	-0,002	0.002	7,332	6,968	7,206	6,653	7,242	7,617	2	31	20	62,4
	AAEL012944	-0,002	0.003	6,207	6,429	6,329	6,278	5,918	6,775	1	5	5	21,1
	AAEL011255	-0,008	0.007	4,968	4,300	5,155	5,106	4,300	5,041	1	3	3	68,9
	AAEL010352	-0,010	0.006	5,179	4,300	5,672	5,409	4,300	5,473	2	8	8	91,0
	AAEL006885	-0,012	0.006	6,293	7,295	5,729	7,358	6,036	5,958	7	9	8	28,2
	AAEL012010	-0,028	0.016	5,596	5,469	4,300	5,535	4,300	5,613	1	2	2	16,4
	AAEL020619	-0,036	0.021	5,336	4,300	5,543	5,663	4,300	5,323	6	3	3	56,4
	AAEL012545	-0,039	0.019	5,057	5,523	5,040	5,534	4,300	4,904	1	5	5	29,0
	AAEL008166	-0,042	0.018	5,263	4,300	5,273	6,362	4,300	4,300	1	3	3	35,3
	AAEL012062	-0,045	0.024	5,524	4,300	5,680	5,809	4,300	5,529	24	7	7	110,9
	AAEL012904	-0,045	0.017	4,991	5,751	4,300	6,578	4,300	4,300	1	8	8	49,9
	AAEL028043	-0,046	0.014	6,378	4,300	6,827	6,647	4,300	6,698	2	6	6	17,0
Piwi5	AAEL012323	-0,048	0.025	5,586	4,300	5,613	5,455	4,300	5,887	1	7	7	105,7
	AAEL027978	-0,055	0.070	4,795	4,300	5,049	5,406	4,300	5,296	1	2	2	219,2
	AAEL006912	-0,060	0.033	4,970	5,141	4,300	5,991	4,300	4,300	2	5	5	41,0
	AAEL012943	-0,061	0.046	5,174	4,300	5,271	5,354	4,300	5,275	1	3	3	48,6
	AAEL008481	-0,066	0.023	6,135	4,300	6,404	6,394	4,300	6,342	2	7	7	22,0
	AAEL013989	-0,083	0.085	4,898	4,300	5,145	5,400	4,300	4,300	1	2	2	10,3
	AAEL015064	-0,101	0.043	4,929	5,530	4,300	6,462	4,300	4,300	1	3	3	10,9
	AAEL005997	-0,108	0.044	5,134	5,456	4,300	6,615	4,300	4,300	2	7	7	14,8
	AAEL005269	-0,109	0.057	4,300	5,521	4,300	5,847	4,300	4,300	2	3	3	45,5
	AAEL019408	-0,119	0.045	5,725	6,048	4,300	6,772	4,300	5,356	1	6	5	21,9
	PLAK_HUMAN	-0,119	0.145	5,483	5,900	6,141	5,489	6,143	6,250	10	11	11	81,7
	AAEL018211	-0,125	0.176	4,789	4,300	4,716	5,052	4,300	4,828	1	3	3	195,1
	AAEL003130	-0,134	0.078	5,446	4,300	5,505	5,657	4,300	5,697	4	3	3	26,6
	AAEL014583	-0,136	0.126	6,233	7,156	6,010	6,239	6,776	6,791	2	3	3	11,3
	AAEL007765	-0,150	0.088	4,300	5,336	5,785	4,300	4,300	5,299	7	4	4	42,4
	AAEL003957	-0,150	0.049	5,905	6,625	4,300	7,089	5,890	4,300	2	7	7	17,1
	AAEL000454	-0,164	0.104	5,463	4,300	5,265	5,669	4,300	5,550	2	3	3	38,8
	AAEL010340	-0,166	0.160	4,300	4,300	5,224	4,964	4,300	5,057	3	2	2	20,4
	AAEL002539	-0,167	0.111	4,935	4,300	4,700	5,836	4,300	4,300	2	7	7	78,1
	AAEL014562	-0,169	0.251	6,889	7,333	6,593	6,853	7,074	7,392	1	4	4	17,6
	AAEL023255	-0,170	0.100	4,843	5,202	4,548	6,181	4,300	4,622	2	9	9	95,7
	K1C16_HUMA	-0,187	0.350	6,895	6,884	7,157	6,760	7,370	7,368	1	29	15	51,3
	AAEL005544	-0,192	0.157	5,178	4,300	5,056	5,390	4,300	5,421	5	3	3	93,3
	AAEL000424	-0,202	0.171	4,300	4,896	4,300	5,502	4,300	4,300	1	2	2	54,9
	AAEL006833	-0,203	0.154	4,854	4,300	4,535	5,698	4,300	4,300	2	4	4	34,5
	AAEL007707	-0,211	0.140	4,300	5,123	4,300	5,757	4,300	4,300	2	3	3	35,7
	AAEL002886	-0,236	0.135	4,300	5,270	4,300	5,979	4,300	4,300	4	3	3	54,0
	AAEL008687	-0,242	0.401	6,670	7,007	7,023	7,025	6,819	7,583	3	12	12	41,6
	AAEL006634	-0,249	0.190	5,129	4,300	5,128	5,705	4,300	5,299	1	3	3	43,3
	K1C14_HUMA	-0,253	0.442	6,505	6,513	6,882	6,471	7,165	7,023	1	24	10	51,6
	AAEL011746	-0,321	0.210	4,9									